



Preparation and thermoelectric power properties of highly doped p-type Sb₂Te₃ thin films

A.M. Adam^{a,*}, E.M. Elsehly^b, M. Ataalla^c, A. El-Khouly^{b,d}, Ayman Nafady^{e,**}, A.K. Diab^a

^a Physics Department, Faculty of Science, Sohag University, Sohag, 82524, Egypt

^b Damanshour University, Faculty of Science, Physics Department, 22516, Damanshour, Egypt

^c Faculty of Engineering and Technology, Badr University in Cairo (BUC), Badr City, Cairo, Egypt

^d National University of Science and Technology MISIS, Moscow, 119049, Russian Federation

^e Department of Chemistry, College of Science, King Saud University, Riyadh, 11451, Saudi Arabia

ARTICLE INFO

Keywords:

Sb₂Te₃
Thin films
Bi addition
Electrical conductivity
Seebeck coefficient

ABSTRACT

In this study, we provide facile procedures for the growth of p-type Bi-doped Sb₂Te₃ thin films on ceramic substrates using vacuum thermal evaporation technique. Crystal structure and surface morphology of the prepared films were probed via powder X-ray diffraction (PXRD) and scanning electron microscope (SEM). The thermoelectric power properties were investigated, in terms of electrical conductivity and Seebeck coefficient measurements, over the temperature range from room temperature up to 473 K. The electrical conductivity behavior showed notable transition from metallic behavior to semiconducting as a function of temperature. In addition, Seebeck coefficient measurements confirmed this transition and supported the behavior of the electrical conductivity. Importantly, power factor was estimated based on both the electrical conductivity and Seebeck coefficient values. A maximum value of 227.6 μW/m.K² was obtained for the Sb_{1.85}Bi_{0.15}Te₃ thin film sample at 428 K.

1. Introduction

Over the past few decades, thermoelectric power (TEP) materials have been extensively investigated both theoretically and experimentally as a promising technology for resolving contemporary energy and environmental issues [1–6]. These materials have also found the way towards many industrial applications such as solid-state coolers, power generators, and infrared detectors.

In principle, TEP material is a material that can convert thermal energy directly into electrical energy and vice-versa. This conversion is based on three important transport effects: the Seebeck effect, the Peltier effect and the Thomson effect. More importantly, the fabricated thermoelectric devices have the advantages of reliability, silence due to the absence of moving mechanical parts, and environmentally friendly.

Despite the advantages of the TEP materials, the efficiency of based devices is still not high enough for daily life applications. The energy conversion efficiency of a TEP material is given by the dimensionless parameter named as figure of merit (ZT), which is expressed by the equation:

$$ZT = \frac{S^2 \cdot \sigma}{(K_e + K_l)} T \quad (1)$$

where *S* is the Seebeck coefficient [mV/K], σ is the electrical conductivity [$\Omega^{-1} \text{cm}^{-1}$] *K_e* and *K_l* are the electronic and lattice thermal conductivity [$\mu\text{W/cm K}$], respectively.

Since the past decade, smart materials such as superlattices [1,2], Skutterudites [3,4] and nano-structured films [5,6] have been produced to achieve higher values of ZT during a reduction of the lattice thermal conductivity. However, these materials usually require complex and expensive processing technology or have been optimized for use at high temperatures only.

In this context, Sb₂Te₃ is considered as one of the best thermoelectric power materials as it can achieve a relatively high figure of merit at room temperature [7]. Telluride-based alloys have witnessed great interest owing to their potential applications in thermo-power generators and coolers as well as thermal sensors [8,9]. In addition, they can be utilized in energy-related applications such as solar cells and phase-change devices [10]. In particular, thin telluride-based films

* Corresponding author.

** Corresponding author.

E-mail addresses: a.adam@science.sohag.edu.eg, alaa.mohamed@science.sohag.edu.eg (A.M. Adam), anafady@ksu.edu.sa (A. Nafady).

<https://doi.org/10.1016/j.physe.2020.114505>

Received 7 June 2020; Received in revised form 28 September 2020; Accepted 15 October 2020

Available online 21 October 2020

1386-9477/© 2020 Elsevier B.V. All rights reserved.

Article

Preparation, Characterization, and Evaluation of Macrocrystalline and Nanocrystalline Cellulose as Potential Corrosion Inhibitors for SS316 Alloy during Acid Pickling Process: Experimental and Computational Methods

Arafat Toghan ^{1,2} , Mohamed Gouda ^{3,*}, Kamal Shalabi ⁴  and Hany M. Abd El-Lateef ^{3,5,*} 

¹ Chemistry Department, College of Science, Imam Mohammad Ibn Saud Islamic University (IMSIU), Riyadh 11623, Saudi Arabia; arafat.toghan@yahoo.com

² Chemistry Department, Faculty of Science, South Valley University, Qena 83523, Egypt

³ Department of Chemistry, College of Science, King Faisal University, Al Hofuf, Al-Ahsa 31982, Saudi Arabia

⁴ Chemistry Department, Faculty of Science, Mansoura University, Mansoura 35516, Egypt; dr-kamal@mans.edu.eg

⁵ Chemistry Department, Faculty of Science, Sohag University, Sohag 82524, Egypt

* Correspondence: mgoudaam@kfu.edu.sa (M.G.); hmahmed@kfu.edu.sa or hany_shubra@science.sohag.edu.eg (H.M.A.E.-L.)



Citation: Toghan, A.; Gouda, M.; Shalabi, K.; El-Lateef, H.M.A. Preparation, Characterization, and Evaluation of Macrocrystalline and Nanocrystalline Cellulose as Potential Corrosion Inhibitors for SS316 Alloy during Acid Pickling Process: Experimental and Computational Methods. *Polymers* **2021**, *13*, 2275. <https://doi.org/10.3390/polym13142275>

Academic Editors: Muhammad Sohail Zafar and Mohamed Hassan El-Newehy

Received: 7 May 2021

Accepted: 16 June 2021

Published: 12 July 2021

Publisher's Note: MDPI stays neutral with regard to jurisdictional claims in published maps and institutional affiliations.



Copyright: © 2021 by the authors. Licensee MDPI, Basel, Switzerland. This article is an open access article distributed under the terms and conditions of the Creative Commons Attribution (CC BY) license (<https://creativecommons.org/licenses/by/4.0/>).

Abstract: Converting low-cost bio-plant residuals into high-value reusable nanomaterials such as microcrystalline cellulose is an important technological and environmental challenge. In this report, nanocrystalline cellulose (NCC) was prepared by acid hydrolysis of macrocrystalline cellulose (CEL). The newly synthesized nanomaterials were fully characterized using spectroscopic and microscopic techniques including FE-SEM, FT-IR, TEM, Raman spectroscopy, and BET surface area. Morphological portrayal showed the rod-shaped structure for NCC with an average diameter of 10–25 nm in thickness as well as length 100–200 nm. The BET surface area of pure CEL and NCC was found to be 10.41 and 27 m²/g, respectively. The comparative protection capacity of natural polymers CEL and NCC towards improving the SS316 alloy corrosion resistance has been assessed during the acid pickling process by electrochemical (OCP, PDP, and EIS), and weight loss (WL) measurements. The outcomes attained from the various empirical methods were matched and exhibited that the protective efficacy of these polymers augmented with the upsurge in dose in this order CEL (93.1%) < NCC (96.3%). The examined polymers display mixed-corrosion inhibition type features by hindering the active centers on the metal interface, and their adsorption followed the Langmuir isotherm model. Surface morphology analyses by SEM reinforced the adsorption of polymers on the metal substrate. The Density Functional Theory (DFT) parameters were intended and exhibited the anti-corrosive characteristics of CEL and NCC polymers. A Monte Carlo (MC) simulation study revealed that CEL and NCC polymers are resolutely adsorbed on the SS316 alloy surface and forming a powerful adsorbed protective layer.

Keywords: natural polymers; nanocrystalline cellulose; corrosion protection; DFT calculations; green synthesis

1. Introduction

SS316 steel alloy has widespread usage in chemical, automotive, petroleum, and oil production [1]. Its mechanical, physical, and structural characteristics make it appropriate for use as a suitable component, or part the SS316 steel alloy parts might corrode in acidic, alkaline, or neutral mediums [2]. SS316 steel alloy is vulnerable to harsh circumstances such as acidic or saline solutions [3]. Numerous approaches have been applied for the protection of these alloys from serious corrosion issues according to the economic aspects and service type [4–6]. The corrosion is an electrochemical process in which anodic and

PROPERTIES OF PANCHARATNAM PHASE AND ENTANGLEMENT OF A FIVE-LEVEL ATOM INTERACTING WITH A SQUEEZED FIELD

S. Abdel-Khalek,^{1,2*} E. M. Khalil,¹ and Haifa S. Alqannas³

¹*Department of Mathematics and Statistics
Collage of Science, Taif University
P.O. Box 11099, Taif 21944, Saudi Arabia*

²*Department of Mathematics
Faculty of Science, Sohag University
Sohag, Egypt*

³*Department of Physics
Faculty of Science, University of Jeddah
Jeddah, Saudi Arabia*

*Corresponding author e-mail: sayedquantum@yahoo.co.uk

Abstract

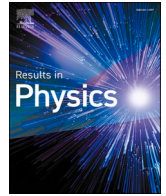
We introduce a quantum scheme where a single five-level atom interacts with a single-mode cavity field by a time-dependent coupling. During the interaction, the temporal behavior of the quantum entropy in the atomic basis is compared with that of the Mandel parameter used to quantify the nonclassical properties of the field. With the field prepared in a squeezed coherent state, the atomic quantum entropy is then used to quantify the entanglement or the nonlocal correlation of the five-level atom (5LA)–field system. The influence of one- and two-photon transitions and the atomic motion on the degree of entanglement and the Pancharatnam phase is analyzed. The analysis emphasizes that both the time dependence and photon multiplicity play an important role in the evolution of the degree of entanglement, the Pancharatnam phase, and nonclassical properties. This insight may be very useful in various applications in quantum physics and quantum optics.

Keywords: five-level atom, linear entropy, atomic motion, squeezing parameter, photon multiplicity.

1. Introduction

Essential features in quantum mechanics, namely, the Pancharatnam phase (PP) and the geometric phase (GP) have been studied by many physicists [1–5]. Michael Berry demonstrated that the quantum object – the wave function (WF) – maintains its evolution in the complex-valued argument of the WF, namely, the GP factor. In regard to its dynamical influence, the GP factor depends on the path geometry of the scheme that the quantum object traverses [6]. This factor is stable despite the uncertainties in control and environmental perturbations. Therefore, researchers pay it close attention while conducting fault-tolerant quantum computations. Focusing on the generalized Heisenberg algebra coherent state (CS), we have recently explored the PP and the purity of the field for several quantum systems [7,8].

In this context, the link between the GP and field purity is highly sensitive to the photon transition number and the initial atomic state. In regard to the atomic motion, the influence of a time-dependent



Properties of transient spectrum and field purity for a qubit system in squeezed states

I.A. Osman^a, K.K. Kabashi^a, S. Abdel-Khalek^{b,c}, K. Berrada^d, Abeer S. Altowyan^e

^a Physics Department, Faculty of Science, Taif University, Taif, Saudi Arabia

^b Mathematics Department, Faculty of Science, Taif University, Taif, Saudi Arabia

^c Mathematics Department, Faculty of Science, Sohag University, Sohag, Egypt

^d Imam Mohammad Ibn Saud Islamic University (IMSIU), College of Science, Department of Physics, Riyadh, Saudi Arabia

^e Department of Physics, College of Science, Princess Nourah bint Abdulrahman University, Riyadh, Saudi Arabia

ARTICLE INFO

Keywords:

Squeezed coherent states
Squeezed number states
Transient spectrum
Field purity

ABSTRACT

The present study investigates the transient spectrum (TS) of a two-level system that interacts with a generalized squeezed state without using the rotating wave approximation (RWA). We consider the purity of the optical field, which is developed in a generalized squeezed state, utilizing the linear entropy. The analytic expressions of the TS and field purity (FP) of the bipartite system are evaluated. Moreover, the study exhibits the influence of the squeezed parameter and some photons transition on the TS and FP. We obtain that the control of the FP may be generated based on an adequate choice of the photons transition and squeezed parameter. Such results can be utilized in the understanding and development of various tasks of quantum physics and optics.

Introduction

The abrupt radiation is considered as a primary reason of energy relaxation in an environmentally-coupled quantum system. However, it can be controlled by changing the field affects the quantum system [1], referred to as the Purcell effect. Enclosing the qubits in a cavity resonator that is detuned from the qubit frequency has resulted in improving the qubit lifetime while keeping qubit control [2–4]. Such dispersive coupling amid the qubit and the resonator plays a role in reducing the channels of decay close to the qubit frequency. However, these channels should undergo additional suppression. Contemporary authors have benefited from these techniques in the mismatches of engineering impedance in the Purcell decay channels existing in the resonator [5,6].

The photon, as a concept, in the quantum theory pertaining to a radiation field relied on the number (Fock) state. Nonetheless, the coherent states are also significant, which are defined as a linear superposition of the Fock states with choosing coefficients. In this case, the states can be generated by acting the displacement operator on the vacuum state [7–9]. Recently, squeezed states have played an important role in the development of various tasks of quantum technology. These states are classified as non-classical states in quantum optics that can be generated by using the operation of the squeezed operator [10]. Squeezed displaced Fock states were developed and their various features, including squeezing and photon statistics were explored [11,12]. They extend two-photon coherent states [13] (squeezed coherent states), squeezed number states [14] and displaced Fock states [15].

Lately, authors have reported the development of motion of a trapped ion in nonclassical states, e.g. Fock states, coherent states, squeezed states and Schrödinger-cat states [16,17].

The JCM (Jaynes Cummings model) has fulfilled the foundation of the nonclassical states through the conditional measurement method [16]. Dakna, Knoll and Welsch (1998) have provided a review for further details relevant to JCM [17]. The development of coherent states with JCM is a significant issue because it provides the information about the non-classical effects that depend on the kinds of the interaction between atoms and fields, including the cases of Schrödinger-cat states [18], displaced number states [19] and squeezed coherent states [20]. It has been shown that the squeezed parameter significantly affects the dynamical properties of the field primarily in the squeezed coherent state [21]. Recent works have shown the effect of the squeezed parameter on the entanglement for a system of two 3LAs (three-level atoms) interacting with a squeezed field [22]. The dynamical properties of a 3LA coupled to a field mode primarily developed in the squeezed coherent state without using the RWA have investigated [23,24]. The effect of the atomic motion within center-of-mass wave functions and atom nanolithography has examined [25]. Recently, the emission spectrum of an optical radiation field interacting with a 2LA when this field is initially in the coherent states (CSs) of added photons associated with pseudo-harmonic oscillators has discussed [26]. Moreover, it has found that the emission spectrum is extremely sensitive to the deformed field and detuning parameters [27]. More recently, a link between the emission spectrum and quantum state fidelity for an atomic system

<https://doi.org/10.1016/j.rinp.2021.104297>

Received 22 October 2020; Received in revised form 2 May 2021; Accepted 4 May 2021

Available online 11 May 2021

2211-3797/© 2021 The Authors.

Published by Elsevier B.V. This is an open access article under the CC BY-NC-ND license

(<http://creativecommons.org/licenses/by-nc-nd/4.0/>).



Radial vibrations on an elastic medium subjected to rotation and magnetic field

G. A. Yahya^a, A. M. Abd-Alla^b, and Sherif El-Bendary^c

^aFaculty of Science, Department of Physics, Aswan University, Aswan, Egypt; ^bFaculty of Science, Department of Mathematics, Sohag University, Sohag, Egypt; ^cFaculty of Science, Department of Mathematics, Tanta University, Tanta, Egypt

ABSTRACT

Based on the one-dimensional elastic theory, the radial vibrations of cylindrical isotropic embedded in an elastic medium are studied in the paper. The effect of the magnetic field of the radial vibrations of an elastic hollow cylinder with rotation is researched as well. The one-dimensional equation of elastodynamic is solved in terms of radial displacement. The frequency equation is obtained when the boundaries are free and fixed; the mixed boundary condition is numerically examined. The determination is concerned with the eigenvalues of the natural frequency of the radial vibrations in the case of harmonic vibrations. The effect of the magnetic field and rotation on the natural frequencies were explored. It was shown that the dispersion curves of guided waves were significantly influenced by the magnetic field and rotation of the elastic cylinder. Numerical results are given and graphically illustrated in each considered case. The natural frequencies and mode shapes are calculated numerically, and the effects of rotating, magnetic field, and variable thickness are discussed. It is observed that an increase of the magnetic parameter, as well as the rotation parameters, brings results closer to the classical cylinder theory results. Furthermore, the current study can be applied to the design of microplates and nanoplates and their optimal usage. The results indicate that the effects of the magnetic field and rotation are very pronounced.

ARTICLE HISTORY




Received 16 December 2020
Accepted 10 January 2021

KEYWORDS

Elastodynamics; radial vibrations; isotropic material; magnetic field; rotation; elastic; hollow cylinder

1. Introduction




In the past, accidental failure of rotating cylinder wheels due to flexural vibration has frequently occurred in rotodynamic machinery such as steam turbines and gas turbines. Wang, Wang, and Liu (2020) investigated the mechanical magnetic coupling vibration instability of an angular rotor subjected to synchronous load in axial-flux permanent magnet motors. Lu, Tsouvalas, and Metrikine (2019) studied the vibration of higher-order model for in plane vibrations of rotating rings on an elastic foundation. Shojaeefard et al. (2018) studied the free vibration problem of an ultra-fast-rotating-induced cylindrical nanoshell resting on a Winkler foundation under a thermo-electro-magneto-elastic condition and recommended some protective measures. Sobhy and Zenkour (2018) investigated the effect of the magnetic field on the thermomechanical buckling and vibration of viscoelastic sandwich nanobeams in humid environment. Zhu et al. (2020) discussed the axisymmetric torsional and longitudinal vibrations for an incompressible SEA cylindrical tube under inhomogeneous biasing fields induced by radial electric voltage and axial pre-

CONTACT G. A. Yahya  Gamal102@yahoo.com  Gamal102@aswu.edu.eg  Faculty of Science, Department of Physics, Aswan University, Aswan 81528, Egypt.
Communicated by Dr Krzysztof Kamil Zur.

© 2021 Taylor & Francis Group, LLC

Article

Regression Models to Estimate Accumulation Capability of Six Metals by Two Macrophytes, *Typha domingensis* and *Typha elephantina*, Grown in an Arid Climate in the Mountainous Region of Taif, Saudi Arabia

Yassin M. Al-Sodany ¹, Muneera A. Saleh ², Muhammad Arshad ³ , Kadry N. Abdel Khalik ^{4,5},
Dhafer A. Al-Bakre ⁶  and Ebrahim M. Eid ^{1,7,*} 

¹ Botany Department, Faculty of Science, Kafrelsheikh University, Kafr El-Sheikh 33516, Egypt; yalsodany@sci.kfs.edu.eg

² Biology Department, College of Science, Taif University, Taif 26571, Saudi Arabia; muneera_salah@hotmail.com

³ Chemical Engineering Department, College of Engineering, King Khalid University, Abha 61321, Saudi Arabia; moakhan@kku.edu.sa

⁴ Biology Department, Faculty of Applied Science, Umm Al-Qura University, Makkah 24243, Saudi Arabia; kadry3000@yahoo.com

⁵ Botany Department, Faculty of Science, Sohag University, Sohag 82514, Egypt

⁶ Biology Department, College of Science, Tabuk University, Tabuk 47512, Saudi Arabia; dalbakre@ut.edu.sa

⁷ Biology Department, College of Science, King Khalid University, Abha 61321, Saudi Arabia

* Correspondence: ebrahim.eid@sci.kfs.edu.eg or eeid@kku.edu.sa or ebrahim.eid@gmail.com; Tel.: +96-65-4574-1874; Fax: +96-61-7241-8205



Citation: Al-Sodany, Y.M.; Saleh, M.A.; Arshad, M.; Abdel Khalik, K.N.; Al-Bakre, D.A.; Eid, E.M. Regression Models to Estimate Accumulation Capability of Six Metals by Two Macrophytes, *Typha domingensis* and *Typha elephantina*, Grown in an Arid Climate in the Mountainous Region of Taif, Saudi Arabia. *Sustainability* **2022**, *14*, 1. <https://doi.org/10.3390/su14010001>

Received: 4 December 2021

Accepted: 13 December 2021

Published: 21 December 2021

Publisher's Note: MDPI stays neutral with regard to jurisdictional claims in published maps and institutional affiliations.



Copyright: © 2021 by the authors. Licensee MDPI, Basel, Switzerland. This article is an open access article distributed under the terms and conditions of the Creative Commons Attribution (CC BY) license (<https://creativecommons.org/licenses/by/4.0/>).

Abstract: In this study, we explored the capacity for two promising macrophytes, *Typha domingensis* and *Typha elephantina*, to be used for the surveillance of contamination by six metals, i.e., Cu, Fe, Mn, Ni, Pb, and Zn, in the mountainous area of Taif City in Saudi Arabia. Regression models were generated in order to forecast the metal concentrations within the plants' organs, i.e., the leaves, flowers, peduncles, rhizomes, and roots. The sediment mean values for pH and the six metals varied amongst the sampling locations for the respective macrophytes, indicating that similar life forms fail to indicate equivalent concentrations. For instance, dissimilar concentrations of the metals under investigation were observed within the organs of the two rooted macrophytes. The research demonstrated that the segregation of metals is a regular event in all the investigated species in which the metal concentrations vary amongst the different plant constituent types. In the current study, *T. domingensis* and *T. elephantina* varied in their capacity to absorb specific metals; the bioaccumulation of metals was greater within *T. domingensis*. The relationships between the observed and model-estimated metal levels, in combination with high R^2 and modest mean averaged errors, offered an appraisal of the goodness of fit of most of the generated models. The *t*-tests revealed no variations between the observed and model-estimated concentrations of the six metals under investigation within the organs of the two macrophytes, which emphasised the precision of the models. These models offer the ability to perform hazard appraisals within ecosystems and to determine the reference criteria for sediment metal concentration. Lastly, *T. domingensis* and *T. elephantina* exhibit the potential for bioaccumulation for the alleviation of contamination from metals.

Keywords: bioaccumulation and translocation factors; bioaccumulators; cattails; environmental pollution; macrophytes; prediction models; wetlands

1. Introduction

Metals are a specific class of elements that, in contrast to organic contaminants, are unable to be broken down via biological processes [1]. Owing to their adverse impact

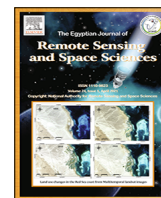
HOSTED BY



ELSEVIER

Contents lists available at ScienceDirect

The Egyptian Journal of Remote Sensing and Space Sciences

journal homepage: www.sciencedirect.com

Remote sensing-based geological mapping and petrogenesis of Wadi Khuda Precambrian rocks, South Eastern Desert of Egypt with emphasis on leucogranite

Asran M. Asran^a, S.M. Hassan^{b,*}^a Geology Department, Faculty of Science, Sohag University, Sohag 82524, Egypt^b National Authority for Remote Sensing and Space Sciences, Cairo, Egypt

ARTICLE INFO

Article history:

Received 7 March 2019

Revised 10 July 2019

Accepted 11 July 2019

Available online 19 July 2019

Keywords:

Leucogranites

Khuda

I-type

Remote sensing

Eastern Desert

Egypt

ABSTRACT

The exposed Precambrian rocks along Wadi Khuda area, South Eastern Desert of Egypt, comprise gneisses, amphibolites and migmatites associations (infrastructural rocks) which are intruded by diorite, tonalite, syenogranite and leucogranite (LG). LG forms homogeneous boss like bodies, devoid to xenoliths, except along the outer margins. Chemically and mineralogically they are dissimilar to the surrounding gneisses. In the current study, band ratio and Decorrelation Stretch image processing algorithms were proposed and applied on Landsat-8, Advanced Spaceborne Thermal Emission and Reflection Radiometer (ASTER) and Sentinel-2 remote sensing data to discriminate the widely exposed lithological units in the mapped area. Geochemically, I-type classification and volcanic arc environment were revealed. LG is peraluminous (ASI average of 1.09) with normative corundum up to 1.38 for LG. The LG displays limited major and trace element variations ($\text{SiO}_2 = 74.5\text{--}76.2\%$, $\text{Al}_2\text{O}_3 = 13.4\text{--}14.4\%$, $\text{MgO} = 0.03\text{--}0.19\%$, $\text{Na}_2\text{O} = 3.6\text{--}4.6\%$, and $\text{Rb} = 55\text{--}85$ ppm) probably due to textural and mineralogical homogeneity. The contents of REE in the leucogranite are low ($\sum\text{REE} = 21\text{--}37$), but the REE patterns are $[(\text{La}/\text{Yb})_n = 2.45\text{--}9.03]$, $[(\text{La}/\text{Sm})_n = 1.09\text{--}2.6]$, with negative Eu anomaly, $(\text{Eu}/\text{Eu}^* = 0.19\text{--}0.78)$. The negative Eu anomaly and the low Sr content (16–92 ppm) may be attributed to the plagioclase feldspars fractionation. The leucogranites represent residual melt of syenogranite which forms Um Itly pluton at the southern flank of Wadi Khuda entrance.

© 2019 National Authority for Remote Sensing and Space Sciences. Production and hosting by Elsevier B.V. This is an open access article under the CC BY-NC-ND license (<http://creativecommons.org/licenses/by-nc-nd/4.0/>).

1. Introduction

The Egyptian granites are differentiated into grey and pink types (e.g. El-Gaby et al., 1988, 1990). The grey (older) granite type was emplaced during the Pan-African Orogeny (i.e. Syn-orogenic) and are of I-type granites (Chappell and White, 1974). The monzogranites and syenogranites were emplaced during post Pan-African event which are referred to the younger (pink) granite type (Late to post orogenic) which is mostly equivalent to A-type granite (Chappell and White, 1974). The S-type granite was proposed to some granites at the Eastern Desert of Egypt e.g. Sikait area (Mohamed and Hassanen, 1997) and the El-Hudi area (Moghazi et al., 2001), where they are distinguished by their chemical and

mineralogical characters (Fig. 1). There are several hypotheses concerning the mode of formation, evolution and tectonic setting of the granitic melts, some of these mechanism considered the interaction between mantle and the lower crust (e.g. Pitcher, 1983). Therefore, the granitic rocks could be formed by anatexis and/or fractional crystallization (FC) processes of lower crust and subduction related magmatism respectively (Stern and Hedge, 1985; Stern and Abdelsalam, 1998; El-Gaby et al., 1990; Fritz et al., 2002; Johnson and Woldehaimanot, 2003; Heikal et al., 2019). Granitic rocks with crustal components have been differentiated from the mantle-derived types in arc-type and/or at an active continental margin (Abdel-Rahman and Martin, 1990).

Remote sensing data such as ASTER, Sentinel-2 and Landsat-8 were used for lithological mapping in the Eastern Desert of Egypt (e.g. Gabr, et al., 2015; Hassan and Ramadan, 2015; Hassan, et al., 2015; Hassan and Sadek, 2017; Hassan et al., 2017; Ali-Bik, et al., 2018).

Peer review under responsibility of National Authority for Remote Sensing and Space Sciences.

* Corresponding author.

E-mail address: safaa.hassan@narss.sci.eg (S.M. Hassan).

<https://doi.org/10.1016/j.ejrs.2019.07.004>

1110-9823/© 2019 National Authority for Remote Sensing and Space Sciences. Production and hosting by Elsevier B.V.

This is an open access article under the CC BY-NC-ND license (<http://creativecommons.org/licenses/by-nc-nd/4.0/>).



Reservoir Formation Damage; Reasons and Mitigation: A Case Study of the Cambrian–Ordovician Nubian ‘C’ Sandstone Gas and Oil Reservoir from the Gulf of Suez Rift Basin

Ahmed E. Radwan^{1,2} · David A. Wood³ · A. M. Abudeif⁴ · M. M. Attia⁴ · M. Mahmoud⁵ · Ahmed A. Kassem² · Maciej Kania¹

Received: 13 September 2020 / Accepted: 14 July 2021
© The Author(s) 2021

Abstract

Reservoir formation damage is a major problem that the oil and gas industry has to mitigate in order to maintain the oil and gas supply. A case study is presented that identifies the impacts of formation damage and their causes in the Nubian ‘C’ hydrocarbon reservoir within Sidki field located in the Southern Gulf of Suez, Egypt. In addition, a formation damage mitigation program was designed and implemented involving an effective stimulation treatment for each well experiencing reservoir damage. The data available for this study include core analysis to provide rock mineralogy and lithology; analysis of production fluid data; water chemistry; drilling fluid composition; perforations and well completion details; workover operations; and stimulation history. The diagnosis of formation damage based on the integrated assessment of the available data is associated with several benefits, (1) The integration of the data available helps provide a robust analysis of formation damage causes and in establishing suitable remediation actions, (2) Workover fluid is confirmed as the primary cause of reservoir damage in the studied well, (3) Several reservoir damage mechanisms were identified including water blockage, solids and filtrate invasion, fluid/rock interaction (deflocculation of kaolinite clay), salinity shock and/or high-sulfate content of the invaded fluid, (4) Irrespective of the potential causes of formation damage, the primary objective of a gas production company is to mitigate its effects and the integrated dataset helps to design appropriate and effective stimulation treatments to overcome formation damage, and (5) In gas reservoirs, especially low permeability ones, extra precautions are necessary to avoid potential reservoir damage due to workover fluid invasion.

Keywords Reservoir damage analysis · Formation damage · Reservoir damage reasons · Reservoir damage mitigation · Nubia sandstone reservoir · Gas reservoir · Workover Formation damage · Fines migration · Well stimulation · Fluid invasion · Water blockage · Overbalanced workover · Integrated formation damage assessment workflow

✉ Ahmed E. Radwan
radwanae@yahoo.com

¹ Faculty of Geography and Geology, Institute of Geological Sciences, Jagiellonian University, Gronostajowa 3a, 30-387 Kraków, Poland

² Gulf of Suez Petroleum Company (GUPCO), Cairo, Egypt

³ DWA Energy Limited, Lincoln, UK

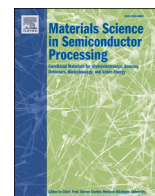
⁴ Geology department, Faculty of Science, Sohag University, Sohag, Egypt

⁵ Petroleum Engineering Department, King Fahd University of Petroleum & Minerals, Dhahran, Saudi Arabia

1 Introduction

Formation or reservoir damage is a challenging issue in oil and gas industry that can substantially reduce fluid flow rates and recovery from subsurface reservoirs [1–6]. It typically involves the reduction in the near-wellbore permeability leading to a reduction in the well productivity. It is a relatively frequent outcome of operations conducted on wellbores during drilling, workover, production, stimulation programs and/or other actions designed to enhance gas or oil recovery (EOR) [3–10]. Many authors have investigated the potential causes of formation damage, and a number of distinct potential causes have been identified in relation to the various downhole activities carried out in gas and oil boreholes [ex 3, 4, 6, 11–30]. Reservoir damage involves





Role of Cu dilute on microstructures, optical, photoluminescence, magnetic and electrical properties of CdS film

Meshal Alzaid^{a,**}, Mohrah Alwshih^a, Mohamed N. Abd-el Salam^b, N.M.A. Hadia^{a,c,*}

^a Physics Department, College of Science, Jouf University, Al-Jouf, Sakaka, P.O. Box 2014, Saudi Arabia

^b Higher Institute for Engineering and Technology, El-Minya, 61768, Egypt

^c Physics Department, Faculty of Science, Sohag University, 82524, Sohag, Egypt

ARTICLE INFO

Keywords:

Thin films
CdS_{1-x}Cu_x films
Microstructural parameters
Optical parameters
PL spectra
Hysteresis loop
Electrical properties

ABSTRACT

Thin films of CdS_{1-x}Cu_x (with $0 \leq x \leq 0.10$) were deposited using electron beam evaporation. Using XRD, EDX, SEM and UV-Vis-NIR spectroscopy, the impact of [Cu]/[S] on the film properties was examined. The influences of various concentrations of Cu are also elucidated on the optical parameters of the films. The XRD analysis shows that the thin films of CdS_{1-x}Cu_x have been improved and have hexagonal polycrystalline structure with the increase of Cu doping ratio. Additionally, the crystallite size is reduced while the micro-strain ϵ increases with enhancement of the incorporation of Cu in CdS lattice. The envelope method was used to extract the optical parameters of the undoped and Cu-doped CdS films. With the increase of Cu concentration, the energy optical bandgap decreased, and the variation values of band gap could play an important role in solar cell applications. Another optical parameters such as, dissipation factor and real/imaginary dielectric constant parts were evaluated and demonstrated a strong Cu doping dependence. The shift observed in the photoluminescence spectra emission band confirmed Cu's substitution to CdS lattice. The measurements of magnetization using vibrating sample magnetometer illustrated a hysteresis loop in Cu-doped CdS films, and confirmed the room temperature ferromagnetism. Finally, the Hall effect results show that the pure CdS film corresponds to an n-type semiconductor with a resistivity of $8.11 \times 10^{-2} \Omega \text{ cm}$ and a carrier concentration of $29.6 \times 10^{19} \text{ cm}^{-3}$, and the CdS:Cu film is a p-type semiconductor and the resistivity is reduced from 6.8×10^{-2} to $3.7 \times 10^{-2} \Omega \text{ cm}$, and the carrier concentration is reduced from 26.4×10^{19} to $4.1 \times 10^{19} \text{ cm}^{-3}$, which has potential application prospects in solar cells.

1. Introduction

Semiconductor group II – VI doped with transition metals as cobalt (Co), vanadium (V) manganese (Mn), copper (Cu), etc, are essential for their fundamental role of in solar cells manufacture and advanced research materials and technological applications [1,2]. Among these, CdS is very important semiconductor that providing energy gaps of 2.57 eV (in hexagonal phase and 2.42 eV (in cubic phase) at room temperature (RT). In addition, these semiconductors materials possess the interesting properties which qualify them to be utilized in recent different optoelectronic applications such as lasers, visible-light emitting diodes, non-linear optics and modern solar cells of high efficiency [3,4].

Doping CdS semiconducting materials with Cu impurities could lead

to large variations of the resistivity, band gap energy, photo-electrical properties and also altering the type of semiconductor from “n-type to p-type” [5,6]. In fact, the presence of copper atoms in semiconductors are affected many interesting physico-chemical properties and reduce electrical resistance as Cd-S thin films have very high electrical resistance (10^7 – $10^8 \Omega \text{ cm}$) [7,8]. On the other side, the optical properties of doped nano-materials vary from the corresponding host nano-materials as the dopants form deep trap levels serve as luminescence centers. Just a few reports have been published on Cu²⁺ doped Cd-S nanoparticles [9, 10]. As mentioned above, the semiconducting materials doped with a low amount of metal impurities have unique properties that make them important materials for potential applications, yet another purpose is to enhance the optical properties of Cd-S film doping with metal ions. The CdS and CdS:Cu thin films have been prepared by several growth

* Corresponding author. Physics Department, Faculty of Science, Sohag University, 82524, Sohag, Egypt.

** Corresponding author.

E-mail addresses: mmalzaidd@ju.edu.sa (M. Alzaid), nomery_abass@science.sohag.edu.eg (N.M.A. Hadia).

<https://doi.org/10.1016/j.mssp.2021.105687>

Received 1 September 2020; Received in revised form 10 January 2021; Accepted 11 January 2021

Available online 17 January 2021

1369-8001/© 2021 Published by Elsevier Ltd.



Cite this: *Environ. Sci.: Processes Impacts*, 2021, 23, 1006

Sea urchin-like calcium borate microspheres and synergistic action with cholinesterase-inhibiting insecticides for ecofriendly *Spodoptera littoralis* control†

Mohamed Khairy, ^{*,a} Haytham A. Ayoub, ^{ab} Farouk A. Rashwan^a and Hanan F. Abdel-Hafez^b

The development of nanoagrochemicals has attracted much attention in the last decade to overcome the recent agricultural and environmental challenges associated with the intensive usage of insecticides. Herein, nanostructured calcium borate materials with hierarchical sea urchin-like microspheres and microblocks have been synthesized by a facile hydrothermal method. The insecticidal activity of CaB_2O_4 and its synergistic combination with cholinesterase-inhibiting insecticides are explored against *Spodoptera littoralis* (*S. littoralis*) for the first time via a feeding bioassay protocol. The insecticidal efficacy of sea urchin-like microspheres (CB-A) is estimated to be $\text{LC}_{50} = 207 \text{ mg L}^{-1}$ which is two-fold higher than that of microblocks (CBM-A) with $\text{LC}_{50} = 406 \text{ mg L}^{-1}$ after eleven days of exposure. The synergistic combination of the CB-A sample with methomyl and chlorpyrifos increases the toxicity to 2.4 and 2.6-fold higher than that of the individual insecticides, respectively. Significantly, sea urchin-like CaB_2O_4 microspheres cause physical damage to the external insect's cuticle layer, which consequently enhances the uptake of organic insecticides. Our results revealed that calcium borate micro-/nano-structures can be employed as a multifunctional nanoagrochemical in various agricultural programs for *S. littoralis* control and decrease the usage of cholinesterase-inhibiting insecticides.

Received 22nd March 2021
Accepted 14th May 2021

DOI: 10.1039/d1em00125f

rsc.li/espi

Environmental significance

Sea urchin-like CaB_2O_4 microspheres have been synthesized by a facile hydrothermal approach. The insecticidal activity of CaB_2O_4 and its synergistic combination with cholinesterase-inhibiting insecticides *i.e.* methomyl and chlorpyrifos against *Spodoptera littoralis* are explored for the first time. CaB_2O_4 showed high insecticidal activity not only on the larvae stage but also on pupa and adult stages. The combination of CaB_2O_4 with methomyl and chlorpyrifos increased the toxicity to 2.4 and 2.6-fold higher than that of the individual insecticides, respectively. CaB_2O_4 with a sea urchin-like morphology causes physical damage to the cuticle layer and enhances the penetration of organic insecticides and consequently the loss of water content. Our results revealed that calcium borate with a sea urchin-like morphology can be employed as a multifunctional nanoagrochemical in various agricultural programs for *S. littoralis* control and decrease the usage of cholinesterase-inhibiting insecticides.

1. Introduction

Spodoptera littoralis (Boisduval) (Lepidoptera: Noctuidae) is one of the foremost phytophagous damaging insects in Egypt and Africa due to its high generative rate. It feeds on forty plant families and at least eighty-seven different plant species. Several cultivated plants and crops such as cotton, maize, potatoes, cereals, vegetables, and ornamental plants are extensively devastated.¹ Although *S. littoralis* is native to Africa, it spreads

all over the world. Therefore, the European and Mediterranean Plant Protection Organization (EPPO) registered *S. littoralis* as an A2 quarantine pest and alerted it as a highly invasive species in the United States.² Carbamates and organic phosphorus compounds (OPs) are well-known organic insecticides widely used for *S. littoralis* control due to inhibiting the cholinesterase enzyme activity that is responsible for the proper function of an insect's nervous system.³ However, the intensive application of organic insecticides increases the public awareness of their severe risk to human health and the environment. As a result, the Environmental Protection Agency (EPA) banned several organic insecticides.^{4,5} Many researchers and agrochemical companies devoted their interest to developing efficient and sustainable strategies for insect control.⁶ Due to the nano-science revolution, engineering nanomaterials might provide

^aChemistry Department, Faculty of Science, Sohag University, Sohag, 82524, Egypt

^bPlant Protection Research Institute, A. R. C., Nadi El-Said Street – Dokki, Giza, 12311, Egypt. E-mail: mohamed.khairy@science.sohag.edu.eg; Tel: +20 (02) 01092099116

† Electronic supplementary information (ESI) available. See DOI: 10.1039/d1em00125f

RESEARCH

Open Access



Seasonal shape variations, ontogenetic shape changes, and sexual dimorphism in a population of land isopod *Porcellionides pruinosus*: a geometric morphometric study

Tarek G. Ismail

Abstract

Background: Isopods shape features are sensitive and respond to several selective pressures which may result in variations of these features. These pressures might reflect the heterogeneity of the environment where an animal lives. Land isopods *Porcellionides pruinosus* were collected from an agricultural field. Landmarks geometric morphometrics was applied to evaluate its shape changes during two different seasons. The present work aims to (i) assess and characterize morphological changes in body shape of *P. pruinosus* as a response to seasonal variations, (ii) determine differences in the body shape during ontogeny, (iii) examine the effect of intraspecific allometry to interpret the observed variations in the species, and (iv) clarify whether the body shape of *P. pruinosus* can be used as a sexual differentiating trait.

Results: Juveniles showed no seasonal variations in the body shape, which were detected among adults, females and males as shown by PCA, DFA, and MANOVA.

The adult winter forms have large bodies, small heads, broad pereons, and short but wide telsons. The adult summer forms have small slender bodies, slightly stretched heads, and relatively long telsons. Juveniles' growth to adulthood showed body shape changes in the head and pereon, that include shrank of the head in the anteroposterior direction and its level became slightly lower than the body. The pereon becomes broader and the two anterolateral projections of the first pereonite extend anteriorly, reaching a little beyond the posterior margin of the eyes. Present species showed a shape sexual dimorphism which includes the broader body and more convex pereon in females and a small waist between the second and third pleonites in males. Shape sexual dimorphism was attributed to reproductive activity. Both allometric trajectories of juveniles and adults (ontogenetic allometry) and of sexes (static allometry) were parallel.

Conclusions: The landmark geometric morphometric technique was able to reveal the seasonal shape variations in terrestrial isopod *P. pruinosus*. Also, this method provides information about shape variations between juveniles and adults, as well as about shape sexual dimorphism.

Keywords: Isopoda, Body shape variations, Geometric morphometric, Seasonal effects, Ontogeny, Sexual dimorphism

Correspondence: t_gad_2000@sohag.edu.eg
Zoology Department, Faculty of Science, Sohag University, P.O. Box 82524,
Sohag, Egypt



© The Author(s). 2021 **Open Access** This article is licensed under a Creative Commons Attribution 4.0 International License, which permits use, sharing, adaptation, distribution and reproduction in any medium or format, as long as you give appropriate credit to the original author(s) and the source, provide a link to the Creative Commons licence, and indicate if changes were made. The images or other third party material in this article are included in the article's Creative Commons licence, unless indicated otherwise in a credit line to the material. If material is not included in the article's Creative Commons licence and your intended use is not permitted by statutory regulation or exceeds the permitted use, you will need to obtain permission directly from the copyright holder. To view a copy of this licence, visit <http://creativecommons.org/licenses/by/4.0/>.



Secondary minerals in a calcareous environment: an example from Um Gheig Pb/Zn mine site, Eastern Desert, Egypt

Mostafa Redwan¹ · Dieter Rammlmair² · Khulan Berkh²

Received: 25 August 2020 / Accepted: 15 March 2021 / Published online: 25 March 2021
© The Author(s), under exclusive licence to Springer-Verlag GmbH Germany, part of Springer Nature 2021

Abstract

Alteration of abandoned mine sites and wastes generates variable secondary mineral phases that incorporate different toxic trace elements with a prospective threat to the neighboring ecosystems. The main focus of this study was to investigate the mineralogical and geochemical changes at neutral pH where dry condition prevails around oxidation-primary contacts interface and the surface in Um Gheig Pb/Zn mine, Eastern Desert, Egypt. The secondary minerals were determined by M4 Tornado μ -EDXRF, Raman microscope and scanning electron microscopy with energy-dispersive system. Two alteration zones were recognized depending on ion availability and the Eh/pH conditions. The first include anglesite as an initial phase that quickly transformed into a more stable cerussite and hydrocerussite. Mendipite formation was controlled by the availability of Cl^- ions in the solution. Hemimorphite was formed after sphalerite in the pore spaces, depending on the accessibility of Si ions from silicates dissolution. Iron (oxy) hydroxides were formed in a later stage due to their restricted mobility in carbonates. The second zone includes gypsum and anhydrite formed at the surface of the mine wastes due to continuous evaporation in arid environments. These secondary mineral phases can undergo different mineral transformations depending on the prevailing conditions. The element release ratios in the mine surface zone compared to the capillary fringe zone reached 12.1, 2.8, 1.6, 0.17, 0.09 and 0.03 for Sr, Cr, Pb, Zn, Cu, and Ni in the mine surface zone compared to 5.86, 0.01, 0.05, 0.02, 0.07 and 0.01 in the capillary fringe zone. The findings from this investigation have important implications for the management and the control of elements mobility from secondary phases formed in mined areas.

Keywords Mine wastes · Secondary minerals · Arid environments · Pb/Zn mine · Eastern Desert · Egypt

Introduction

Abandoned mining sites cause many environmental issues to the nearby soil and surface/groundwater resources worldwide (Younger et al. 2002; Khelifaoui et al. 2020). After mining operations cease, pyrite (FeS_2) and other metal sulfides located in the mine wastes undergo oxidation after exposure to atmospheric oxygen. The oxidation mechanism depends on many factors including the mineralogy and reactivity of sulfides and carbonates, the particle size, porosity and surface area, the climate including the temperature and water content, the Eh/pH conditions and microbiological

activity (Nordstrom and Alpers 1999; Rammlmair et al. 2008; Redwan et al. 2012; Oyewo et al. 2018). Mine wastes can generate after oxidation acidic water rich in different metals, which are potential eco-toxicants (Jambor 1994). If carbonate is present, the acidity is buffered by carbonate minerals dissolution, resulting in co-precipitation of secondary mineral phases (Blowes and Ptacek 1994; Oyewo et al. 2018) depending on the chemical constitution of the primary wastes and the prevailed conditions. The secondary minerals act as sinks for toxic trace elements and remove them by precipitation (e.g., as hydroxides), coprecipitation, or surface-reactive iron (oxy) hydroxides or sorption onto organic material (Dzombak and Morel 1990; España et al. 2005; Alakangas and Öhlander 2006; Schaidler et al. 2014).

Natural attenuation mechanisms by absorption and precipitation of toxic trace elements or valuable economic trace elements that can accumulate as amorphous or micro-to crystalline phases within tailings and waste materials (Graupner et al. 2007; Rammlmair et al. 2008; Redwan et al.

✉ Mostafa Redwan
mostafa.redwan@science.sohag.edu.eg

¹ Geology Department, Faculty of Science, Sohag University, Sohag 82524, Egypt

² BGR Hannover, Stilleweg 2, 30655 Hannover, Germany

**PHYSICS OF NUCLEI
AND ELEMENTARY PARTICLES**

Sensitivity of Polarization Observables in $\gamma d \rightarrow \pi^0 d$ Reaction Near Threshold to the Choice of Elementary $\gamma N \rightarrow \pi N$ Amplitude and Deuteron Wave Function

E. M. Darwish^{1*} and H. M. Al-Ghamdi²

¹*Physics Department, Faculty of Science, Sohag University, Sohag 82524, Egypt*

²*Physics Department, College of Science, Princess Nourah bint Abdulrahman University, P. O. Box 84428, Riyadh 11671, Saudi Arabia*

Received January 03, 2021; revised February 28, 2021; accepted March 11, 2021

Abstract—We study the sensitivity of polarization observables in $\gamma d \rightarrow \pi^0 d$ reaction near threshold to the choice of elementary $\gamma N \rightarrow \pi N$ amplitude and NN potential model adapted for the deuteron wave function (DWF). Numerical results for various beam, target, and beam–target polarization observables are presented and systematic uncertainties caused by the use of different elementary operators and DWFs are evaluated. The calculations are based on a $\gamma d \rightarrow \pi^0 d$ approach in which realistic models for the elementary pion production amplitude and the DWF are used. We find considerable dependencies of the estimated results for all possible polarization observables on the elementary amplitude. The spin asymmetries Σ , T_{21}^c , T_{10}^l , and T_{20}^l show large sensitivities to the DWF. In contrast, the asymmetries T_{11} , T_{2M} ($M = 0, 1, 2$), T_{10}^c , and E as well as the helicity difference $d(\sigma^P - \sigma^A)/d\Omega$ have slight dependence on the DWF only at photon energies very close to π -threshold. The unpolarized differential cross section is also predicted and compared with the available experimental data, and a satisfactory agreement is obtained only at forward pion angles. We expect that the results presented here may be useful to interpret the recent measurements from Jefferson Lab, TAPS@ELSA, A2 and GDH@MAMI Collaborations.

Keywords: meson production, photoproduction reactions, few-body systems, deuteron, polarization phenomena in reactions, spin observables, polarized beams, polarized targets.

DOI: 10.3103/S0027134921030036

1. INTRODUCTION

Meson electromagnetic production on light nuclei is of fundamental interest and thus constitute a major topic in medium energy nuclear physics with respect to the following important reasons: (i) used to investigate the structure of hadrons in the nonperturbative domain of quantum chromodynamics (QCD) and therefore the nature of strong interactions, (ii) study of the behavior of nucleon resonances in the nuclear medium, (iii) yields important information about πN and NN interactions as well as the electromagnetic properties of elementary particles, (iv) gives complementary information on pion production on off-shell nucleons which is important for the study of pion production on all other nuclei as well, (v) provides us with a wealth of important information about the role of the nuclear environment on the elementary amplitudes,

and (vi) serves as a test of our understanding of the chiral πN dynamics.

Coherent pion photoproduction on the deuteron is worth to be studied, since relevant experimental studies are performed [1–30]. This process may be used as an isospin filter and it is sensitive to the coherent sum of the proton and neutron amplitudes $\gamma p \rightarrow \pi^0 p$ and $\gamma n \rightarrow \pi^0 n$, respectively. The use of deuteron as an effective neutron target allows one to obtain abundant information about the mechanisms of the elementary pion photoproduction on the free neutron which otherwise is not possible due to the absence of any free neutron targets. Furthermore, the deuteron represents also an ideal object for the study of NN interactions.

During the last decades, coherent π^0 -photoproduction on the deuteron has been studied extensively in the photon lab-energy region from π -threshold up to 1 GeV as a source of information on π^0 -photoproduction off the neutron [31–62]. Despite all

*E-mail: darwish@science.sohag.edu.eg



Simultaneous biodegradation of harmful *Cylindrospermopsis raciborskii* and cylindrospermopsin toxin in batch culture by single *Bacillus* strain

Zakaria Mohamed¹ · Saad Alamri² · Mohamed Hashem^{2,3}

Received: 25 January 2021 / Accepted: 16 August 2021 / Published online: 21 August 2021
© The Author(s), under exclusive licence to Springer-Verlag GmbH Germany, part of Springer Nature 2021

Abstract

This study investigates the capability of a *Bacillus flexus* strain isolated from decayed cyanobacterial blooms for the bioremediation of *Cylindrospermopsis raciborskii* and cylindrospermopsin (CYN) toxin. The algicidal activity of this strain was tested by co-cultivation with *C. raciborskii* cultures. CYN biodegradation was investigated in the presence of living and heat-inactivated bacterial cells or bacterial filtrate. Living bacterial cells inhibited *C. raciborskii* growth after 2 days of incubation with complete cell death at day 5. Bacterial filtrate caused a rapid reduction in *C. raciborskii* growth at the first day, with complete cell lysis at day 3. Only living cells of SSZ01 caused reduction in CYN released into the medium during the bacterial decay of *C. raciborskii* cells. The biodegradation rate of CYN by SSZ01 relied on initial toxin concentrations. The highest rate ($42 \mu\text{g CYN L}^{-1} \text{ day}^{-1}$) was obtained at the higher initial concentration ($300 \mu\text{g L}^{-1}$), and the lowest ($4 \mu\text{g CYN L}^{-1} \text{ day}^{-1}$) was at lower concentration ($50 \mu\text{g L}^{-1}$). These results suggest that this bacterial strain could be employed to bioremediate cyanobacterial blooms in freshwaters. Also, the application of this bacterium in slow sand filters would give possibilities for degradation and bioremediation of cyanotoxins in drinking water treatment plants.

Keywords Bacteria · Biodegradation · Biological control · *Cylindrospermopsis* · Cylindrospermopsin · Lysis

Highlights

- We proved the lytic activity of *Bacillus flexus* SSZ01 against *C. raciborskii*
- The lytic activity was mediated by bacterial secretion of active metabolites
- Strain SSZ01 can also degrade CYN toxin released from decayed cyanobacterial cells
- This strain could be used as a bioagent to control *C. raciborskii* bloom in water
- The strain could be applied in slow sand filters to remove CYN from drinking water

Responsible Editor: Vitor Vasconcelos

✉ Zakaria Mohamed
zakaria.attia@science.sohag.edu.eg; mzakaria_99@yahoo.com

¹ Faculty of Science, Department of Botany and Microbiology, Sohag University, Sohag 82524, Egypt

² Department of Biology, King Khalid University, College of Science, Abha 61413, Saudi Arabia

³ Faculty of Science, Botany and Microbiology Department, Assiut University, Assiut 71516, Egypt


Introduction

Harmful cyanobacterial blooms (HCBs) seriously threaten the environmental and human health. HCBs are a common phenomenon in freshwater environments worldwide, and they may increase in the future because of progressive eutrophication of aquatic ecosystems and climate change (Paerl and Otten 2013). Most cyanobacterial blooms are constituted by toxin-producing species which damage the aquatic ecosystem and impair the safety of drinking water (Mohamed and Al-Shehri 2007; Mohamed et al. 2015). Among bloom-forming cyanobacteria, *C. raciborskii* is one of the most common and widespread species, and characterized by geographic expansion due to its high plasticity and physiological tolerance to a wide range of environmental conditions, e.g., light, temperature, and nutrients (Padisak 1997; Burford and Davis 2011). Additionally, *C. raciborskii* can produce hepatotoxins (e.g., cylindrospermopsin) and neurotoxins (saxitoxins) that have been implicated in fish, domestic livestock, and human mortalities (Svircev et al. 2016).

CYN is an alkaloid toxin with a low molecular weight (415Da), inhibiting protein synthesis (Van Apeldoorn et al.



Structural, optical and electrical properties of $\text{Bi}_{2-x}\text{Mn}_x\text{Te}_3$ thin films

N. M. A. Hadia^{1,2,*} , S. H. Mohamed^{3,4}, W. S. Mohamed¹, Meshal Alzaid¹, Mohd Taukeer Khan³, and M. A. Awad⁴

¹Department of Physics, College of Science, Jouf University, Jouf, Kingdom of Saudi Arabia

²Basic Sciences Research Unit, Jouf University, Jouf, Kingdom of Saudi Arabia

³Department of Physics, Faculty of Science, Islamic University of Madinah, Prince Naifbin Abdulaziz, Al Jamiah, Madinah 42351, Kingdom of Saudi Arabia

⁴Physics Department, Faculty of Science, Sohag University, Sohag 82524, Egypt

Received: 17 July 2021

Accepted: 21 October 2021

Published online:
1 November 2021

© The Author(s), under exclusive licence to Springer Science+Business Media, LLC, part of Springer Nature 2021

ABSTRACT

Undoped and Mn doped Bi_2Te_3 ($x = 0, 0.05$ and 0.10 at%) thin films were prepared via thermal evaporation method from their bulk alloys. X-ray diffraction revealed the presence of hexagonal Bi_2Te_3 crystalline phase only in all undoped and Mn doped films. EDAX quantitative analysis revealed that the effective Mn doping is close to that of the intended. SEM observations revealed uniform spherical grains for all films with more porous and less dense grains at higher Mn content. The increase in Mn doping ratio to $x = 0.1$ decreases the carrier density and the carrier type changes to the P-type conduction. The transmittance values increased with Mn doping whereas the reflectance decreased. The optical band gap increased from 0.25 to 0.39 eV. Two layer-model was successfully used to simulate the ellipsometry measurements. The main layer was described by a combined contribution of Drude and Lorentz models. The thickness, the optical constants, and the surface roughness of the undoped and Mn doped films were extracted from the ellipsometry measurements. Upon Mn doping, the PL was quenched.

1 Introduction

Bismuth Telluride (Bi_2Te_3) is one of the most important thermoelectric semiconductor materials which have been utilized in devices fabrication such as thermoelectric generators [1], flexible thermoelectric devices [2], thermoelectrics in sequencing reactions and driving DNA amplification [3], photodetector in

harsh working environments [4], thin film Hall bar device [5] and transducer for solar energy [6].

Doping of Bi_2Te_3 with transition metal is an active field of research due to the change in properties that can be tailored by the doping level and the numerous applications which can be utilized [7–10]. Mn doped Bi_2Te_3 films are no exception. One of the important effects is the layered crystal structure of Mn doped

Address correspondence to E-mail: nmhadia@ju.edu.sa

Structure Explication, Biological Evaluation, DNA Interaction, Electrochemistry and Antioxidant Activity of Iron (II) tri- and Tetra-Dentate Schiff base Amino Acid Complexes

Ahmed M. Abu-Dief*, Laila H. Abdel-Rahman, Emad F. Newair and Nahla Ali Hashem

Chemistry Department, Faculty of Science, Sohag University, Sohag 82534, Egypt.

Received: 7 Jan. 2021, Revised: 2 Apr. 2021, Accepted: 17 Apr. 2021.

Published online: 1 May 2021

Abstract: New azomethine Schiff base amino acid ligands derived from the condensation reaction of 3-methoxysalicylaldehyde (MS) or 4-diethylaminosalicylaldehyde (DS) with some of α -amino acids (L-phenylalanine (Phe), L-histidine (His), DL-tryptophan (Trp)) and their Fe(II) complexes were prepared. Structures of the synthesized Fe(II) complexes were determined on the basis of elemental analysis, infrared, ultraviolet-visible spectra, thermal analysis and cyclic voltammetry (CV) as well as conductivity, magnetic susceptibility measurements. Moreover, the particle size distribution of the prepared complexes was determined by using transmittance electron microscope (TEM). The experimental results show that the investigated Fe(II) complexes contain hydrated water molecules (except DSPFe complex) and coordinated water molecules (only in MSHFe complex). The kinetic and thermal parameters were determined from the thermal data using Coast and Redfern method. The results suggest that MS or DS amino acid Schiff bases behave as monobasic tridentate ONO ligands and coordinate to Fe(II) in octahedral geometry according to the general formula $[\text{Fe}(\text{HL})_2] \cdot n\text{H}_2\text{O}$. But in the case of MSHFe complex, MSH ligand acts as tetradentate $(\text{NH}_4^+)[\text{Fe}(\text{HL})(\text{H}_2\text{O})\text{SO}_4] \cdot 2\text{H}_2\text{O}$. The conductivity values between $43.30\text{--}5.66 \Omega^{-1} \text{mol}^{-1} \text{cm}^{-2}$ in DMF suggest the presence of non-electrolyte species, except MSHFe complex is electrolyte species ($60.3 \Omega^{-1} \text{mol}^{-1} \text{cm}^{-2}$). Moreover, the antimicrobial evaluation of the prepared Schiff base amino acid ligands and their Fe(II) complexes was examined against three types of bacteria such as *B. subtilis* (+ve), *E. coli* (-ve) and *M. luteus* (+ve) and three types of fungi such as *A. niger*, *C. glabrata* and *S. cerevisiae*. The results of these studies signaling that the metal chelates exhibit a stronger antimicrobial efficiency than their corresponding ligands. Moreover, the interaction of the prepared Fe(II) complexes with (CT-DNA) by using spectral studies, viscosity measurements and agarose gel electrophoresis was investigated. Furthermore, antioxidant activities of the synthesized complexes were examined by using the ABTS assay and showed that the prepared complexes have a good antioxidant activity.

Keywords: Amino acid, Fe(II) complexes, Antimicrobial, Cyclic voltammetry, antioxidant, DNA interaction.

1 Introduction

There are few amino acids which are principles for human beings such as: phenylalanine, tryptophan, and histidine. They are very much necessity, as they cannot be bio-synthesized by our body. Phenylalanine: Helps in boosting memory power and helps to maintain a healthy nervous system. Tryptophan: Plays a vital role in maintaining our appetite. Histidine: Helps in the yielding and synthesis of both RBC (red blood cells) and WBC (white blood cells).

Phenylalanine is important in the construction of

structural proteins in tissue. The concentrations of phenylalanine govern the amounts of other electrically neutral amino acids in the brain. Tryptophan catabolism in cancer is progressively more being identified as a marked microenvironmental factor that curbs antitumor immune responses. It has been suggested that the fundamental amino acid tryptophan is catabolized in the tumor tissue by the rate-restrictive enzyme indole amine-2, 3-dioxygenase (IDO) revealed in tumor cells or antigen-presenting cells [1]. Tryptophan is the only amino acid bound to plasma albumin [2]. Part of the tryptophan bound to albumin is available for uptake into the brain

* Corresponding author E-mail: ahmed_benzoic@yahoo.com



Contents lists available at ScienceDirect

Optik

journal homepage: www.elsevier.com/locate/ijleo

Original research article

Study the effect of type of substrates on the microstructure and optical properties of CdTe Thin Films

A.M. Abdel Hakeem^a, H.M. Ali^a, M.M. Abd El-Raheem^a, M.F. Hasaneen^{a,b,*}^a Physics Department, Faculty of Science, Sohag University, 82524, Sohag, Egypt^b Physics Department, College of Science, Jouf University, Al-Jouf, Sakaka, P.O. Box 2014, Sakaka, Saudi Arabia

ARTICLE INFO

Keywords:

CdTe
thin films
microstructure
refractive index
optical energy gap

ABSTRACT

Cadmium telluride (CdTe) thin films are deposited on an ultrasonically cleaned substrate of different types by using thermal evaporation technique under pressure 2×10^{-5} mbar. The structural and morphological studies of all the films are accomplished using the X-ray diffraction method (XRD) and field emission scanning electron microscope (FE-SEM). CdTe found to have a polycrystalline structure. The grains were very uneven and the grain shape was irregular. A Jasco V-570 UV- visible - NIR spectrometer has been used to measure the optical properties in the range of wavelength from 200 to 2500 nm at normal incidence. The optical energy gap (E_g) is determined by using the Tauc's equation. The optical parameters such as; refractive index (n), static refractive index (n_0), infinite dielectric constant (ϵ_∞), dispersion energy (E_d), single oscillating energy (E_0), static dielectric constant (ϵ_s), free carrier concentration (N), plasma frequency (ω_p), relaxation time (τ), oscillator wavelength (λ_o), oscillator strength (S_0) and electronic polarizability (α_p) respectively are calculated. The optical measurements for CdTe films deposited on FTO substrate were properly used as absorber material for solar cell applications. Inversely, CdTe films deposited on a glass substrate is more suitable for a window in solar cell applications.

1. Introduction

In the latest years, Cadmium Telluride (CdTe) semiconductor is a compound with potential applications for using in photovoltaics of solar cells [1,2], optoelectronic devices such as detectors [3,4] and p-n junction devices [5]. It has Zinc blende crystal structure. CdTe is unique among II-VI compounds which make it important and quite suitable for several applicants as it may exhibit both n-type and p-types conductivity [6–8]. Otherwise, CdTe shows the p-type semiconductor because of the Cd vacancies rare present. CdTe is a direct band gap semiconductor and has an optimal width of the band gap of 1.5 eV, which is a suitable difference in the energy range for converting solar radiation into electricity [9,10]. So, CdTe thin films of thickness $1 \mu\text{m}$ found to have a high optical absorption coefficient and absorption of about 10^4 cm^{-1} , 92% respectively of the visible light [11]. This absorption value belongs to CdTe is better than that of crystalline silicon, which needs about $200 \mu\text{m}$ to reach the same value [12].

Several methods are used for the preparation of thin films of CdTe such as Sputtering [13,14], spray pyrolysis [3], close space vapor transport, metal-organic chemical vapor deposition and thermal evaporation [15–17]. Among the major advantages of thermal evaporation technique high deposition rates, relative simplicity, and low cost of the equipment must be mentioned. This process uses a strong vacuum environment, and so is capable of producing very high purity thin films [18–20].

* Corresponding author.

E-mail address: moh_f_2001@yahoo.com (M.F. Hasaneen).<https://doi.org/10.1016/j.ijleo.2020.165390>

Received 5 March 2020; Received in revised form 17 July 2020; Accepted 3 August 2020

Available online 7 August 2020

0030-4026/© 2020 Elsevier GmbH. All rights reserved.



Synergistic inhibition effect of novel counterion-coupled surfactant based on rice bran oil and halide ion on the C-steel corrosion in molar sulphuric acid: Experimental and computational approaches



Hany M. Abd El-Lateef^{a,b,*}, Mai M. Khalaf^{a,b,*}

^a Department of Chemistry, College of Science, King Faisal University, P.O. Box 400, Al-Ahsa 31982, Saudi Arabia

^b Department of Chemistry, Faculty of Science, Sohag University, Sohag 82524, Egypt

ARTICLE INFO

Article history:

Received 29 December 2020

Received in revised form 19 February 2021

Accepted 25 February 2021

Available online 27 February 2021

Keywords:

Counterion-coupled surfactant

Surface morphology

Synergism

Corrosion protection

Green synthesis

DFT

ABSTRACT

The counterion-coupled surfactant (RBOS-12) based on rice bran oil is synthesized, characterized, and evaluated as a new inhibitor for carbon steel corrosion. The inhibition, and synergistic effect performance of individual RBOS-12, and that is combined with chloride ions on the corrosion of carbon steel in a molar sulphuric acid medium at $30\text{--}60 \pm 1$ °C has been examined using open circuit potential-time, linear polarization resistance (LPR) corrosion rate, impedance spectroscopy (EIS), potentiodynamic polarization (PDP), surface topology (Field emission-scanning electron microscopy/Energy dispersive X-ray analysis (FE-SEM/EDS), X-ray diffraction (XRD) and UV-vis spectroscopic studies), density functional theory (DFT) and molecular dynamics (MD) simulations. Experimental findings exhibited that the inhibition capacity of individual RBOS-12 is 95.5% at the concentration of 1.0×10^{-3} M. Synergistic inhibition effect was observed between the RBOS-12 surfactant and the Cl⁻ ion additives, with the maximum corrosion inhibition capacity as high as ~99.1% at 1×10^{-5} M RBOS-12 + 0.1 M Cl⁻ ions. The individual RBOS-12 and RBOS-12/Cl⁻ system get adsorbed onto the metal interface through mixed categories of adsorption mainly with the chemisorption. Meanwhile, the adsorption mode follows the Langmuir isotherm model. FE-SEM/EDS and XRD investigates approve the protective and adsorption capabilities of the individual RBOS-12 and RBOS-12/Cl⁻ inhibitor systems. UV-vis spectroscopic analysis display that the additive interacts with metal in H₂SO₄ medium to form Fe-inhibitor complexes. DFT calculations and MD simulations further support the empirical outcomes. The findings exhibited that the prepared RBOS-12/Cl⁻ system can be used as economic, eco-friendly, and efficient corrosion inhibitor with good anticorrosion properties for metals in acidic environments.

© 2021 Elsevier B.V. All rights reserved.

1. Introduction

Carbon steel (C-steel) has been considered as one of the most significant and usually utilized in innumerable engineering and manufacturing applications, including automotive, petroleum, water and power generation, chemical treating and a diversity of other manufacturing. The significance and extensive utilize of C-steel is related to its low-cost and outstanding mechanical-chemical characteristics [1,2]. Nevertheless, one of the major dilemmas of using C-steel is its susceptibility to corrosion in various corrosive solutions predominantly mineral acids for instance H₂SO₄ and HCl [3]. One of the efficient and essential tools to impede the C-steel corrosion in mineral acids is the application

of inhibitors, which diminishes the aggression of solutions towards C-steel surfaces [4].

Eco-friendly organic inhibitors applications are emerged to touch the environmental restrictions demands. So, inorganic inhibitors (such as phosphates, chromates, nitrates, and molybdates) that are extremely used in corrosion protection of metal/alloys (e.g., C-steel) are substituted despite their high capacity [5–8]. A survey of the previous studies on acid corrosion inhibitors indicates that most of the well-recognized additives contain N, S, and O atoms with N-containing carbon-based compounds as effective inhibitors in hydrochloric acid medium and those with S-containing compounds as effective inhibitors in sulphuric acid solution [9–13]. Compounds containing both N and S could deliver outstanding corrosion inhibition capacity compared with inhibitors containing either S or N [14,15]. The presence of larger electronegative atoms, like N and S, etc., in the inhibitor molecule is found to affect the inhibitor adsorption over corroding metal surface reinforcement efficient inhibition [16]. Organic surfactants, besides their eco-friendly and biodegradable properties they have excellent corrosion protection characteristics. They have high

* Corresponding authors at: Department of Chemistry, College of Science, King Faisal University, P.O. Box 400, Al-Ahsa 31982, Saudi Arabia.

E-mail addresses: hmahmed@kfu.edu.sa, hany_shubra@science.sohag.edu.eg (H.M. Abd El-Lateef), mmkali@kfu.edu.sa (M.M. Khalaf).


 Cite this: *RSC Adv.*, 2021, 11, 2905

Synthesis and antimicrobial activity of some novel 1,2-dihydro-[1,2,4]triazolo[1,5-*a*]pyrimidines bearing amino acid moiety†

 Mounir A. A. Mohamed, ^a Adnan A. Bekhit, ^{*bcd} Omyma A. Abd Allah,^a Asmaa M. Kadry,^a Tamer M. Ibrahim, ^e Salma A. Bekhit,^f Kikuko Amagase^g and Ahmed M. M. El-Saghier^{*a}

A new series of [1,2,4]-triazole bearing amino acid derivatives **2a–d–9a–d** were synthesized under green chemistry conditions *via* multicomponent reaction using lemon juice as an acidic catalyst. The obtained compounds were characterized by different spectral and elemental analyses. The obtained candidates showed promising antibacterial activity against some standard bacteria and multidrug resistant (MDR) clinical isolates. In contrast to the reference drugs cephalothin and chloramphenicol, the tested compounds showed substantial better MIC values towards the tested MDR strains. The most active compounds **3c**, **8a** and **9d** against MDR bacteria were tested for MBC and MIC index, the results indicated the bacteriostatic activity of these compounds. The most active compounds **2c**, **2d**, **3c**, **8a**, **8b**, **9a**, **9b**, **9c** and **9d** showed a high selectivity index towards antimicrobial activity against *K. pneumoniae* and *MRSA1* compared to mammalian cells, suggesting a good safety profile.

Received 24th September 2020

Accepted 29th December 2020

DOI: 10.1039/d0ra08189b

rsc.li/rsc-advances

1. Introduction

Facing emerging bacterial infections has become more challenging worldwide due to the increasing number of multidrug-resistant (MDR) microbes.^{1–7} This indicates the crucial need to develop new efficient anti-bacterial agents. Many factors contribute to mutations in microbial genomes leading to resistance to known antibiotics. For instance, it is broadly confirmed that the abuse of antibiotics can significantly increase the development of resistant-genotypes.^{8–10} As the number of infectious diseases and multidrug-resistant bacterial strains continues to increase, researchers are prompted to develop novel anti-microbial molecules.¹¹

From a medicinal chemistry prospective, creating new generation of therapeutic molecules with improved pharmacological properties and drug-tolerance profile, as well as fewer side effects, is an ultimate goal.¹² Hence, libraries with privileged heterocyclic scaffolds are frequently utilized in the development of new potent drugs.¹³ For instance, hybrids from 1,2,4-triazole derived compounds usually hold a series of pharmacological properties such as anticancer,^{14,15} antiviral,¹⁶ antitubercular,^{17,18} antifungal,¹⁹ antileishmanial²⁰ and antibacterial²¹ activities. However, only few reports about fused systems of 1,2,4-triazolo[1,5-*a*]pyrimidines were reported in literature with pronounced antibacterial activities.²² In addition, coupling with simple amino acids, *e.g.*, glycine and others, has been frequently attracted the interest of medicinal chemists due to its improving ability for the physicochemical and drug-likeness properties.^{20,23} In addition, glycine and its derivatives appear to be promising safe antimicrobial agents.^{24,25}

Being analogues of DNA purine bases, 1,2,4-triazolo[1,5-*a*]pyrimidines can be regarded as plausible substrates for enzymatic biochemical processes.²⁶ In particular, derivatives of [1,2,4]triazolo-[4,3-*a*]pyrimidines have recently been reported as potential antibacterials.^{27–30} It was reported that series of 1,2,4-triazolo[1,5-*a*]pyrimidines carboxamide derivatives attributed good narrow-spectrum antibacterial activity against *E. faecium* and possessed metabolic stability with low intrinsic clearance. Macromolecular synthesis assays revealed cell-wall biosynthesis as the target of these compounds.²² It is worth mentioning that recently, several 1,2,4-triazolo[1,5-*a*]pyrimidines were synthesized and screened for their antibacterial derivatives as DNA

^aDepartment of Chemistry, Faculty of Science, Sohag University, Sohag, Egypt. E-mail: adnbekhit@hotmail.com; adnbekhit@pharmacy.alexu.edu.eg

^bPharmaceutical Chemistry Department, Faculty of Pharmacy, Alexandria University, Alexandria, Egypt. E-mail: el_saghier@yahoo.com

^cCancer Nanotechnology Research Laboratory (CNRL), Faculty of Pharmacy, Alexandria University, Alexandria 21521, Egypt

^dPharmacy Program, Allied Health Department, College of Health and Sport Sciences, University of Bahrain, Zallaq, Kingdom of Bahrain

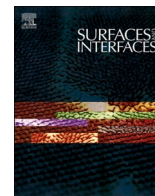
^eDepartment of Pharmaceutical Chemistry, Faculty of Pharmacy, Kafrelsheikh University, Kafrelsheikh 33516, Egypt

^fHigh Institute of Public Health, Alexandria University, Alexandria 21568, Egypt

^gLaboratory of Pharmacology & Pharmacotherapeutics, College of Pharmaceutical Sciences, Ritsumeikan University, Kusatsu, Shiga, Japan

† Electronic supplementary information (ESI) available. See DOI: 10.1039/d0ra08189b





Synthesis and theoretical studies of novel conjugated polyazomethines and their application as efficient inhibitors for C1018 steel pickling corrosion behavior

Hany M. Abd El-Lateef^{a,b,*}, Abdelwahed R. Sayed^{a,c}, K. Shalabi^d

^a Department of Chemistry, College of Science, King Faisal university, P.O. Box 400 Al-Ahsa 31982, Saudi Arabia

^b Chemistry Department, Faculty of Science, Sohag University, Sohag 82524, Egypt

^c Chemistry Department, Faculty of Science, Beni-Suef University, Beni-Suef 62514, Egypt

^d Chemistry Department, Faculty of Science, Mansoura University, Mansoura, Egypt

ARTICLE INFO

Keywords:

Polyazomethines
Inhibition
Surface morphology
Theoretical study
Acidic corrosion

ABSTRACT

The idea of the existing work is to progress the preparation of four conjugated polyazomethines contained thiazole through the backbone of the polymer. The synthesized conjugated polyazomethines were categorized and assessed as novel inhibitors for the C1018 steel pickling corrosion behavior at 298–328 K using surface morphology of C1018 steel electrode, potentiodynamic polarization (PDP), and electrochemical impedance spectroscopy (EIS). The assessed polymers performed as effective inhibitors for C1018 steel corrosion in pickling solution. The protection capacity of the polyazomethines augmented with a rise in concentration to attain 98.2% efficacy with 150 mg L^{-1} at 298 K. PDP plots designated that the conjugated polyazomethines performs as mixed-type inhibitors and adsorbed on the C1018 steel interface via chemisorption. Isotherm model of Langmuir was found the preeminent mode for the adsorption of polymers. The surface morphology examinations established the development of a protective layer getting a thick coverage at the optimal dose. Moreover, theoretical study of Monte Carlo (MC) simulations and density functional theory (DFT) were used to govern the association among protection capacity and molecular structure. This study could be provided novel polyazomethines inhibitors for C1018-steel corrosion protection in different industrial environments, especially in the pickling solution.

1. Introduction

C-steel (carbon steel) has been chosen as unique of the greatest significance and extensively utilized structural accessories in numerous industries, including automotive, chemical processing water, petroleum, and power generation, and a diversity of other applications [1,2]. The wide and important use of C- steel is related to its outstanding mechanical features and low-cost [2,4]. Nevertheless, C-steel is inclined to corrosion in refinery categorized mineral acids such as H_2SO_4 (sulfuric acid), HCl (hydrochloric acid), H_2SO_3 (sulfurous acid), and thio-sulfurous [5]. Among the previous corrosion mediums, hydrochloric acid is generally used in various industrial implementations like acid pickling, industrial cleaning, scale and rust elimination, acidification of oil wells in petrochemical procedures, and oil retrieval at temperatures up to 333 K [6].

With the aim of treat the aggressive attack of these acids, inhibitors are introduced to the corrosive medium, which diminishes the aggressiveness of acids to the C-steel surface. The chemical materials with both inorganic and organic sources have been applied as inhibitors to preserve minerals from harsh solutions [7]. Organic molecules containing hetero-atoms like nitrogen, oxygen and sulfur, and aromatic rings π -electrons are originated to be actually effective in quashing the corrosion of the metal in various mediums [8,9]. Among the carbon-based materials, polymeric corrosion inhibitors are a very wide choice owing to their huge efficient groups and their capability to complex with metal ions at interfaces [10,11]. By covering great surface extents of alloys and metals in the corrosive solutions, these formed pincers effectively “complete” the surface from aggressive ions and molecules attack thus contributing the required inhibition [12]. Additionally, small inhibitor molecules incline to destroy at higher

* Corresponding author .

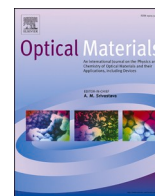
E-mail addresses: hmahmed@kfu.edu.sa, hany_shubra@science.sohag.edu.eg (H.M. Abd El-Lateef).

<https://doi.org/10.1016/j.surfin.2021.101037>

Received 27 December 2020; Received in revised form 28 January 2021; Accepted 17 February 2021

Available online 20 February 2021

2468-0230/© 2021 Elsevier B.V. All rights reserved.



Research Article

Synthesis of an optimized ZnS/Au/ZnS multilayer films for solar cell electrode applications

Mohammed Ezzeldien^{a,b}, Z.A. Alrowaili^c, M.F. Hasaneen^{c,d,*}

^a Department of Basic Sciences, Common First Year Deanship, Jouf University, P.O. Box: 2014, Sakaka, Saudi Arabia

^b Metallurgy & Material Science Tests (MMST) Lab, Department of Physics, Faculty of Science, South Valley University, Egypt

^c Department of Physics, College of Science, Jouf University, Al-Jouf, Sakaka, P.O. Box 2014, Sakaka, Saudi Arabia

^d Thin Films and Nanotechnology Lab, Physics Department, Faculty of Science, Sohag University, 82524, Sohag, Egypt



ARTICLE INFO

Keywords:

ZnS/Au/Zns

Optical bandgap

Swanepoel's involved methods

Refractive index conductive electrodes

ABSTRACT

In this study, different film constructions (ZnS, ZnS/Au, and ZnS/Au/ZnS) were evaporated by thermal evaporation. The study was conducted in order to identify the best film for solar cell applications. The study identifies ZnS (399.6 nm)/Au (18 nm) as the most appropriate film for further investigation because it shows a maximum optical band gap ≈ 3.43 eV and the minimum resistivity ($0.46 \times 10^{-3} \Omega \text{ cm}$). It is noticed that the interference fringes disappeared due to the addition of the Au layer. The absorption edge was shifted towards a lower energy as the Au increased. The band gap E_g and resistivity ρ_{RT} were 3.49 eV and $0.12 \times 10^{-3} \Omega \text{ cm}$ respectively. The refractive index increased up to the maximum value 6.2. The ZnS (399.6 nm)/Au (6 nm)/ZnS (399.6 nm) films exhibited amorphous structure, and with the increase of the Au thickness layer, the diffraction peaks related to FCC phase of the Au appeared. The film ZnS (399.6)/Au 18/ZnS (399.6) shows very promising parameters. The bandgap E_g is 3.38 eV, the sheet resistance is $1.53 \times 10^{-3} \Omega$, the figure of merit equals $3.7 \times 10^{-3} \Omega^{-1}$ and the refractive index is 6.20. The results prove that the film ZnS (399.6)/Au 18/ZnS (399) is suitable for conductive electrodes in solar cells.

1. 1- Introduction

Transparent conduction oxides (TCO's) have been used for the optoelectronic systems applications such as; photovoltaic solar cell, electro-chromic equipment and transistors [1–6]. A synthesis of indium tin oxide, by sputtering, is not easy because of the behavior of indium ions during the diffusion process; high electrical resistivity; scarcity and the high cost of indium resources in nature [7–9]. It is urgently needed to find low cost TCO's for commercial applications [10]. Placing metal between two dielectric layers (dielectric/metal/dielectric (D/M/D)) enhances the reflection of metal in the visible region. This arrangement causes more perfect electrical and optical characteristics than a single layer TCO's [4,11–16]. Extensive attempts have been done mainly on the multi-layers structure, (AZO/Au/AZO [17,18], ITO/Au/ITO [19,20], ZnS/Ag/ZnS [15,16], ZnO/Au/ZnO [21], SnO₂/Ag/SnO₂ [22], ZnO/Cu/ZnO [23] and ZnS/Au/ZnS [24]).

AZO/Au/AZO multi-layers were deposited, by magnetron sputtering, on glass substrate at various Au thicknesses 5–20 nm. Chien Hsun ehu reported that the best values of the mobility and the free carrier

concentration were $1.01 \times 10^{-5} \Omega \text{ cm}$, $2.7665 \text{ cm}^2 \text{ v}^{-1} \text{ s}^{-1}$, and $4.563 \times 10^{22} \text{ cm}^{-3}$ respectively. The transmittance was 86.18% at 650 nm wavelengths at a thickness of 8 nm [17]. Seung jun Lee et al. prepared the AZO/Au (0–12 nm)/AZO multi-layers by atomic layer deposition (ALD) and electron beam evaporation technologies. As the thickness of the Au increases, the free carrier concentration increases to $4.2 \times 10^{21} \text{ cm}^{-3}$. The resistivity decreased from 2.6×10^{-3} to $1.2 \times 10^{-4} \Omega \text{ cm}$ and the transmittance decreased from 80% to 48% [18]. The ITO/Au (10 nm)/ITO multi-layers thin films were deposited on poly-carbonate substrate [19]. For single layer ITO, the free carrier concentration was 7.12×10^{22} and increased to $3.26 \times 10^{22} \text{ cm}^{-3}$ for ITO/Au/ITO [20]. Xuanjie Liu et al. (2001) prepared ZnS/Ag/ZnS nano-multilayers by a thermal evaporation technique. The sheet resistance of ZnS/Ag/ZnS was $3 \Omega/\text{cm}^2$ and the figure of merit F_{TC} was $7.3 \times 10^{-2} \Omega^{-1}$ [25]. The physical properties of the ZnO/Au (3 nm)/ZnO have been studied by H. M. Lee. The transmittance of the thin films decreased because of the addition of Au layer [21]. Caifeng Wang and Bo Hu synthesized ZnS/Au/ZnS multi-layer on quartz glass substrates. They reported that the maximum optical transmittance increases to 86.2% at 200 °C [24].

* Corresponding author. Department of Physics, College of Science, Jouf University, Al-Jouf, Sakaka, P.O. Box 2014, Sakaka, Saudi Arabia.

E-mail addresses: mfahmad@ju.edu.sa, moh_f_2001@yahoo.com (M.F. Hasaneen).

<https://doi.org/10.1016/j.optmat.2021.110814>

Received 17 November 2020; Received in revised form 24 December 2020; Accepted 4 January 2021

Available online 17 January 2021

0925-3467/© 2021 Published by Elsevier B.V.


 Cite this: *RSC Adv.*, 2021, **11**, 17746

Synthesis of highly crystalline LaFeO₃ nanospheres for phenoxazinone synthase mimicking activity†

Mohamed Khairy, * Abdelrahman H. Mahmoud and Kamal M. S. Khalil *

LaFeO₃ nanospheres with an orthorhombic perovskite structure were synthesized by a sol-gel autocombustion method in the presence of different citric acid ratios ($x = 2, 4, 8, \text{ and } 16$) and utilized for the photocatalytic conversion of *o*-aminophenol (OAP) to 2-aminophenoxazine-3-one (APX) for the first time. OAP is one of the most toxic phenolic derivatives used as a starting material in many industries; however, the dimerization product APX has diverse therapeutic properties. Photocatalytic conversion was carried out in ethanol/water and acetonitrile/water mixtures in the absence and presence of molecular oxygen at ambient temperature *via* the oxidative coupling reaction that mimics phenoxazinone synthase-like activity. The LaFeO₃ samples showed a superior photocatalytic activity of OAP to APX with rate constants of 0.43 and 0.92 min⁻¹ in the absence and presence of molecular oxygen, respectively. Thus, the LaFeO₃ nanozymes could be used as promising candidates in industrial water treatment and phenoxazinone synthase-like activity.

 Received 23rd March 2021
 Accepted 28th April 2021

DOI: 10.1039/d1ra02295d

rsc.li/rsc-advances

1. Introduction

Millions of tons of organics are intensively consumed in food additives, pharmaceuticals, pesticides, painting, dyeing, textile industries, and agricultural activities every year. Most of these undesired reagents or starting materials, particularly those called persistent contaminants, are subsequently discharged in the environment and cause serious health risks.¹ Considering the environmental safety issues and energy-effective cost, many restrictions are assessed recently on chemical industries to switch and utilize alternative or greener manufacturing routes. However, large amounts of persistent organic contaminants are still discharged. Biological, thermal, physical, and chemical treatment technologies have been adopted for the mitigation of organics in the last decades.²⁻⁴ Several microorganisms are being utilized to degrade biodegradable organics but the process usually takes a long retention time. Thermal treatment also consumes a large quantity of energy. Membrane separations and adsorption are widely used for removing organic contaminants.^{5,6} Functional materials with large surface areas should be engineered and developed. However, a long separation time and surface regeneration with stable functionality are still major obstacles. Among the aforementioned technologies, chemical oxidation is a promising process for large-scale wastewater treatment under mild conditions. It is usually carried out using chemical reagents, which might be

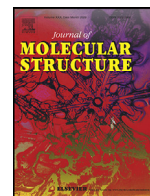
homogenous or heterogeneous processes. Thus, many research works have been devoted to develop both homogenous and heterogeneous catalysts for efficient wastewater treatment.^{7,8}

The photocatalytic oxidation process is an efficient and eco-friendly methodology that utilizes light energy to drive the oxidation reaction, leading to the degradation of organic contaminants to low molecular oxygenated chemical species or the synthesis of new compounds.^{9,10} Irradiation of a semiconductor with a light stimulates the transfer of electrons in the valence band (VB) to the conduction band, leaving behind a positive charge carrier known as a hole.¹¹ These photo-generated charge carriers (e⁻/h⁺) might be recombined again in the bulk catalyst nanoparticles, producing thermal energy or migrating to the catalyst surface. The surface charge carriers can further participate in the catalytic reaction through their redox potentials. The photo-generated hole acts as an electron acceptor in the oxidation processes. Alternatively, the surface adsorbed species such as H₂O molecules and OH⁻ group may trap the photo-generated holes, producing hydroxyl radicals ([•]OH), which is a non-selective strong oxidizing species with a redox potential of 2.80 V (*vs.* NHE). On the other hand, the electrons in the conduction band might reduce the adsorbed O₂ molecules and form superoxide O₂^{•-} radicals. Metal oxides such as TiO₂ and ZnO have been commonly used as heterogeneous photocatalysts.¹² However, their wide energy band gap requires a high photo-energy for excitation. Regrettably, UV irradiation represents only less than 5% of solar energy, which limits these metal oxides' applicability. Accordingly, various attempts have been undertaken to make the photocatalysis process more efficient and economical by utilizing a wide range of visible-light energy.

Chemistry Department, Faculty of Science, Sohag University, 82524, Egypt. E-mail: kms_khalil@yahoo.co.uk; mohamed.khairy@science.sohag.edu.eg; Tel: +20 (2) 01092099116

† Electronic supplementary information (ESI) available. See DOI: 10.1039/d1ra02295d





Synthesis, characterization, molecular modeling and preliminary biochemical evaluation of new copper (II) mixed-ligand complexes

Mohamed Ismael*, Abdel-Mawgoud M. Abdel-Mawgoud, Mostafa K. Rabia, Aly Abdou

Chemistry Department, Faculty of Science, Sohag University, Sohag 82524, Egypt

ARTICLE INFO

Article history:

Received 14 September 2020

Revised 11 November 2020

Accepted 26 November 2020

Available online 1 December 2020

Keywords:

Cu mixed-ligand complexes

Density functional theory (DFT)

Antimicrobial activity

Phenoxazinone synthase-mimicking

Structure activity relationship

ABSTRACT

Three new Cu(II) mixed-ligand complexes of the type [Cu(primary ligand)(secondary co-ligand)], were synthesized, characterized and preliminary tested for their biochemical activities. The primary ligand (HL) was derived from condensation of p-toluidine with 2-hydroxy-naphthaldehyde. Three different N-heterocyclic compounds, 8-hydroxy-quinoline (HQ), 2-(1H-benzimidazol-2-yl)phenol (HB), and 2-(4,5-diphenyl-1H-imidazol-2-yl)phenol (HI), were used as secondary co-ligands. Inhibitory capacity of the synthesized compounds were screened against the growth of pathogenic bacteria [*E. coli* (G⁻) and *B. cereus* (G⁺)] and fungi (*A. fumigatus*), in terms of inhibition zone (IZ, mm), and minimum inhibitory concentration (MIC, $\mu\text{g/mL}$) using the disc diffusion method. Furthermore, the complexes were tested for their phenoxazinone synthase-like activity in terms of K_{cat} . Density functional theory (DFT) calculations based on B3LYP with LanL2DZ level of theory were performed to prove the proposed geometry of the complexes as well as evaluate the electronic parameters responsible for their reactivity. Structure activity relationship formula was derived by correlating the experimental data (MIC or K_{cat}) with the calculated electronic parameters.

© 2020 Elsevier B.V. All rights reserved.

1. Introduction

Copper plays a considerable biochemical role either as an essential trace metal or as a constituent of various external administered compounds in humans. In the former role, it is bound to albumin, and other proteins, while in the latter, it is bound to many ligands forming complexes that interact with biomolecules, mainly proteins and nucleic acids [1]. Current interest in Cu complexes is due to their diverse biological significance as antimicrobial, antiviral, anti-inflammatory, antitumor agents, and enzyme inhibitors [2,3].

The copper-containing metalloenzymes play an important catalytic role in living systems as dioxygen and substrate activators toward different bio-functions, e.g. Phenoxazinone synthase activity [4,5]. Phenoxazinone synthase, is a multicopper oxidase enzyme, found naturally in the bacterium, *Streptomyces* antibiotics, which catalyzes the oxidative coupling of o-aminophenol (OAP) derivatives into phenoxazinone chromophore (Phz). The latter is used clinically for the treatment of Wilm's tumor, gestational choriocarcinoma, and other tumors in which phenoxazinone chromophore is recognized to inhibit DNA-dependent RNA synthesis by intercalation to DNA [6].

There has been enhanced interest in developing new Cu(II) complexes for their biochemical significance. Thus, in the present framework, three Cu(II) mixed-ligand complexes involving a Schiff base as the primary ligand, and N-heterocyclic co-ligand as the secondary one, had been prepared and characterized. Additionally, a preliminary investigation of their *in-vitro* antimicrobial and phenoxazinone synthase-mimicking activity was evaluated. A preliminary screening was undertaken to test their activity efficacies against economically important fungi and bacteria. Firstly, the bare ligands, and their complexes have been evaluated against pathogenic bacteria and fungi that are common contaminants of the environment, and some of which are involved in human and animal diseases, e.g. *Aspergillus fumigatus*, or frequently reported from contaminated soil, water and food substances, e.g. *Escherichia coli* (G⁻) and *Bacillus cereus* (G⁺). Also, their catalytic activity towards the oxidative coupling of OAP had been investigated.

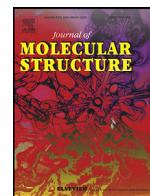
2. Experimental

2.1. Synthesis

All Chemicals used in synthesis of the investigated compounds were of analytical grade and used as received without further purification.

* Corresponding author.

E-mail address: m_ismael@science.sohag.edu.eg (M. Ismael).



Synthesis, crystal structural determination and *in silico* biological studies of 3,3'-ethane-1,2-diylbis(2-benzylidene-1,3-thiazolidin-4-one)



Laila H. Abdel-Rahman^a, Shaaban K. Mohamed^{b,c}, Youness El Bakri^{d,*}, Sajjad Ahmad^e, Chin-Hung Lai^{f,g}, Amer A. Amer^a, Joel T. Mague^h, Ehab M. Abdallaⁱ

^a Chemistry Department, Faculty of Science, Sohag University, Sohag 82524, Egypt

^b Chemistry and Environmental Division, Manchester Metropolitan University, Manchester M1 1GD, England, UK

^c Chemistry Department, Faculty of Science, Minia University, El-Minia 61519, Egypt

^d Department of Theoretical and Applied Chemistry, South Ural State University, Lenin prospect 76, Chelyabinsk 454080, Russian Federation

^e Department of Health and Biological Sciences, Abasyn University, Peshawar 25000, Pakistan

^f Department of Medical Applied Chemistry, Chung Shan Medical University, Taichung 40241, Taiwan

^g Department of Medical Education, Chung Shan Medical University Hospital, Taichung 402, Taiwan

^h Department of Chemistry, Tulane University, New Orleans, LA 70118, USA

ⁱ Chemistry Department, Faculty of Science, New Valley University, Alkharga, Egypt

ARTICLE INFO

Article history:

Received 20 May 2021

Revised 17 June 2021

Accepted 28 June 2021

Available online 14 July 2021

Keywords:

Thiourea

Bis thiourea

Thiazolidinones

Crystal structure

DFT calculations

Molecular docking

Molecular dynamics simulations

ABSTRACT

A new thiazolidine derivative, 3,3'-ethane-1,2-diylbis(2-benzylidene-1,3-thiazolidin-4-one (**4**)) was synthesized and the product obtained was characterized by NMR, IR and mass spectral studies, and the structure was confirmed by single crystal X-ray diffraction studies. The title compound crystallizes in the monoclinic space group $P2_1/n$, the unit cell parameters are $a = 15.9505(8)$ Å, $b = 6.6818(3)$ Å, $c = 18.1799(9)$ Å, $\beta = 94.249(2)^\circ$ and $Z = 4$ at 150 K. In the title molecule, $C_{20}H_{18}N_4O_2S_2$, the thiazolidine rings adopt a "pincer" conformation with the phenylimino substituents extending outwards on both sides. A layer structure is formed in the crystal by C–H...N and C–H...O hydrogen bonds. A Hirshfeld surface analysis was used to explore the nature of the intermolecular interactions in the crystal structure employing molecular surface contours and 2D fingerprint plots have been used to examine molecular shapes. The frontier orbital analysis shows that **4** should be more sensitive to a nucleophilic attack than an electrophilic attack. Molecular docking, followed by molecular dynamics simulation and MM-GBSA binding free energy was carried out to predict the binding affinity of **4** for α -amylase enzyme. These analyses revealed good intermolecular stability of the complex with stable high affinity intermolecular complex formation of high equilibrium nature.

© 2021 Elsevier B.V. All rights reserved.

1. Introduction

Thiazolidine scaffold compounds exhibit notable medicinal and pharmaceutical properties. In the thiazolidine structure, a major number of replacements are suitable on the 2, 4, and 5 positions for improving the component's medicinal importance. Thiazolidine and thiazolidinone are key components of many natural products and drugs. They exist in many synthetic compounds such as antitumor [1,2], anticancer [3–6], antimicrobial [7–9], anti-diabetic [10], anti-inflammatory [11–13], antiparasitic [14,15], antitubercular [16], antiviral [17, 18], antifungal [19], anti-HIV [20–22], antitrypanosomal [23], cytotoxic [24], antinociceptive and anti-hypernociceptive compounds [25].

Also, thiazolidine derivatives are used as an inhibitor of tyrosyl-DNA phosphodiesterase I [26] and influenza neuraminidase [27], as radioprotective agents against γ -irradiation [28], as pro-drugs for the treatment of cystinosis [29], and as S1P1 receptor agonists [30,31]. They are also used in protein chemical synthesis [32], peptide and protein modification [33], as activators to innate immunity [34] and, also act as immune-stimulating agents [35].

Thiazolidine derivatives participate in several syntheses as potential biomarkers for oxidative stress and formaldehyde exposure [36]. They are also used as synthetic precursors, as heterogeneous catalysts [37,38] and as free radical, superoxide anion radical, and hydroxyl radical scavengers [39–41].

Herein, we report the synthesis and characterization of new 3,3'-ethane-1,2-diylbis(2-benzylidene-1,3-thiazolidin-4-one). Foremost, an analysis by single-crystal X-ray diffraction has been undertaken to reach a fine description of the architecture of

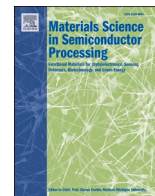
* Corresponding author.

E-mail address: yns.elbakri@gmail.com (Y. El Bakri).



Contents lists available at ScienceDirect

Materials Science in Semiconductor Processing

journal homepage: <http://www.elsevier.com/locate/mssp>

Synthesis, structural and photophysical properties of mixed Zn:SnO₂ nanowires

S.H. Mohamed^{a,b,*}, Mohd Taukeer Khan^a, Abdullah Almohammed^a, M.A. Awad^b

^a Department of Physics, Faculty of Science, Islamic University of Madinah, Prince Naifbin Abdulaziz, Al Jamiah, Madinah, 42351, Saudi Arabia

^b Physics Department, Faculty of Science, Sohag University, 82524, Sohag, Egypt

ARTICLE INFO

Keywords:

Zn:SnO₂ mixed oxide nanowires
XRD
SEM
Optical properties
Photoluminescence

ABSTRACT

The present work demonstrates the structural and photophysical properties of mixed zinc tin oxide (Zn:SnO₂) nanowires (NWs) synthesized via vapor transport technique with Zn content of 10, 25 and 50 wt%. The XRD spectra reveals the tetragonal phase of SnO₂ for 10 wt% Zn content, whereas a combination of tetragonal SnO₂ and hexagonal ZnO phases were observed for higher Zn ratios. The SEM images reveals the formation of smooth NWs for low Zn content, whereas a combination of NWs along with spherical nanoparticles have been observed for 50 wt% Zn:SnO₂ sample. The optical band gap was decreased from 3.21 eV (10% Zn:SnO₂) to 2.84 eV (50% Zn:SnO₂), whereas the corresponding Urbach energy increased from 971 meV to 1132 meV. The refractive index values increased from 2.28 to 2.64 when Zn content increased from 10 to 50 wt%. The absorption spectra showed a red shift and the appearance of new band with increasing Zn wt.%, signaling the formation of new electronic states below the conduction band. The fabricated films displayed a broad steady state emission with peak around 462 nm, which intensity decreased with the increasing of Zn ratio. The effective life time of charge carrier was decreased from 198 ps for 10 wt% Zn:SnO₂ to 172 ps for 50 wt% Zn:SnO₂.

1. Introduction

Tin oxide (SnO₂) nanostructures is an excellent semiconducting material characterized by various admirable photophysical properties including high transparency, high mobility, wide band gap (~ 3.6 eV) and deep energy levels [1]. Moreover, SnO₂ is abundance in nature, environmental friendly, high chemical and mechanical strength and can be synthesized at low temperature [2–6]. Owing to oxygen vacancy and free carries, it can be either n-type or p-type, as well as can be highly reflective in near-infrared (NIR) spectral region. Further, the properties of SnO₂ nanostructures can be easily controlled by varying growth methods and conditions [7–9]. In particular, SnO₂ NWs are characterized by many features such as high surface to volume ratio, high stability and the possibility of syntheses using cost effective methods [10].

These excellent properties led to applications of SnO₂ in various fields such as gas sensors [4,11,12], biosensors [13], catalysis [14], electrode material in energy storage devices [15], photo-thermal shielding coating [16], light emitting diodes [17], etc. Moreover, recently SnO₂ has emerges as alternate of TiO₂ in perovskites solar cells and device based on it have achieved power efficiency in excess of 22%

[18]. Although SnO₂ nanostructures show excellent properties but still there is scope to upgrade its optical and electrical properties. Various strategies including UV irradiation [19], metal doping [20], ion-implantation [21], *n-p* heterojunctions [22] have been adopted for optimization and improvement of SnO₂ nanostructure properties.

Metal doping/mixing is the most common strategy used to optimize the properties of SnO₂ nanostructure [23]. However, metal doping of SnO₂ NWs via vapor transport technique is not an easy task. Zinc (Zn) is among the most popular dopants which are used to achieve the improved electron transport properties of SnO₂ nanostructures [7]. The substitution of Sn ions by Zn lead to formation of broken bonds in the structure which act as acceptor energy states above the valance band. These energy states enhance the concentration of holes in valance band by accepting the electrons from there, provides additional paths for the recombination of conduction band electrons through the valance band hole and enhance the luminescence properties [24]. Due to photo-physical, chemical and the thermal stability of zinc oxide (ZnO), recent investigations showed the enhanced photocatalytic activities [25,26], sensing properties [26], magnetic properties [27], and photoluminescence [28,29] of mixed Zn:SnO₂ nanostructure.

* Corresponding author. Department of Physics, Faculty of Science, Islamic University of Madinah, Prince Naifbin Abdulaziz, Al Jamiah, Madinah, 42351, Saudi Arabia.

E-mail addresses: abo_95@yahoo.com, s.h.Mohamed@science.sohag.edu.eg (S.H. Mohamed).

<https://doi.org/10.1016/j.mssp.2020.105573>

Received 29 September 2020; Received in revised form 5 November 2020; Accepted 12 November 2020

1369-8001/© 2020 Elsevier Ltd. All rights reserved.

Article

Taxonomic Revisiting and Phylogenetic Placement of Two Endangered Plant Species: *Silene leucophylla* Boiss. and *Silene schimperiana* Boiss. (Caryophyllaceae)

Ahmed EL-Banhawy ^{1,*}, Iman H. Nour ^{2,*}, Carmen Acedo ³, Ahmed ElKordy ^{3,4}, Ahmed Faried ^{5,6},
Widad AL-Juhani ^{7,8}, Ahmed M. H. Gawhari ⁹, Asmaa O. Olwey ⁵ and Faten Y. Ellmouni ¹⁰

- ¹ Botany and Microbiology Department, Faculty of Science, Suez Canal University, 41522 Ismailia, Egypt
 - ² Botany and Microbiology Department, Faculty of Science, Alexandria University, 21511 Alexandria, Egypt
 - ³ Biodiversity and Environment Management Department, Faculty of Biological and Environmental Sciences, University of León, 24071 León, Spain; c.acedo@unileon.es (C.A.); aelkordy@science.sohag.edu.eg (A.E.)
 - ⁴ Botany and Microbiology Department, Faculty of Science, Sohag University, 82524 Sohag, Egypt
 - ⁵ Botany and Microbiology Department, Faculty of Science, Assiut University, 71515 Assiut, Egypt; ahmedfaried55@aun.edu.eg (A.F.); asmaa_olwey@science.aun.edu.eg (A.O.O.)
 - ⁶ Biology Department, College of Science and Arts, Sajir, Shaqra University, 11961 Shaqra, Saudi Arabia
 - ⁷ Biology Department, Faculty of Applied Science, Umm Al-Qura University, 24381 Makkah, Saudi Arabia; wsjuhani@uqu.edu.sa
 - ⁸ Research Laboratories Centre, Faculty of Applied Science, Umm Al-Qura University, 24381 Makkah, Saudi Arabia
 - ⁹ Botany Department, Faculty of Science, University of Benghazi, 1308 Benghazi, Libya; ahmed.gawhari@gmail.com
 - ¹⁰ Botany Department, Faculty of Science, Fayoum University, 63514 Fayoum, Egypt; fy100@fayoum.edu.eg
- * Correspondence: ahmedbanhaway@science.suez.edu.eg (A.E.-B.); iman-hassan@hotmail.com (I.H.N.)



Citation: EL-Banhawy, A.; Nour, I.H.; Acedo, C.; ElKordy, A.; Faried, A.; AL-Juhani, W.; Gawhari, A.M.H.; Olwey, A.O.; Ellmouni, F.Y. Taxonomic Revisiting and Phylogenetic Placement of Two Endangered Plant Species: *Silene leucophylla* Boiss. and *Silene schimperiana* Boiss. (Caryophyllaceae). *Plants* **2021**, *10*, 740. <https://doi.org/10.3390/plants10040740>

Academic Editor: Paula Baptista

Received: 13 March 2021

Accepted: 6 April 2021

Published: 9 April 2021

Publisher's Note: MDPI stays neutral with regard to jurisdictional claims in published maps and institutional affiliations.



Copyright: © 2021 by the authors. Licensee MDPI, Basel, Switzerland. This article is an open access article distributed under the terms and conditions of the Creative Commons Attribution (CC BY) license (<https://creativecommons.org/licenses/by/4.0/>).

Abstract: The genus *Silene* L. is one of the largest genera in Caryophyllaceae, and is distributed in the Northern Hemisphere and South America. The endemic species *Silene leucophylla* and the near-endemic *S. schimperiana* are native to the Sinai Peninsula, Egypt. They have reduced population size and are endangered on national and international scales. These two species have typically been disregarded in most studies of the genus *Silene*. This research integrates the Scanning Electron Microscope (SEM), species micromorphology, and the phylogenetic analysis of four DNA markers: ITS, *matK*, *rbcl* and *psb-A/trn-H*. Trichomes were observed on the stem of *Silene leucophylla*, while the *S. schimperiana* has a glabrous stem. Irregular epicuticle platelets with sinuate margin were found in *S. schimperiana*. Oblong, bone-shaped, and irregularly arranged epidermal cells were present on the leaf of *S. leucophylla*, while *Silene schimperiana* leaf has “tetra-, penta-, hexa-, and polygonal” epidermal cells. *Silene leucophylla* and *S. schimperiana* have amphistomatic stomata. The Bayesian phylogenetic analysis of each marker individually or in combination represented the first phylogenetic study to reveal the generic and sectional classification of *S. leucophylla* and *S. schimperiana*. Two *Silene* complexes are proposed based on morphological and phylogenetic data. The *Leucophylla* complex was allied to section *Siphonomorpha* and the *Schimperiana* complex was related to section *Sclerocalycinae*. However, these two complexes need further investigation and more exhaustive sampling to infer their complex phylogenetic relationships.

Keywords: endangered; endemic; *Silene*; SEM; stomata; molecular systematics; phylogenetic analysis; nrDNA ITS; cpDNA *matk*; *Siphonomorpha*; *Sclerocalycinae*

1. Introduction

Caryophyllaceae contain 70–86 genera and 2200 species, which are distributed all over the world [1]. The family is divided into four subfamilies: Alsinoideae, Caryophylloideae, Paronychioideae, and Polycarpoideae “Polycarpaoideae” [2]. Within the Caryophylloideae, the tribe Sileneae DC. is regarded as the largest tribe in the family [3].



Taxonomic Significance of the Leaf Geometric and Micrometric Attributes in the Discrimination of Some Cultivars of *Mangifera indica* L. (Anacardiaceae)



Ahmed EL-Banhawy^{(1)#}, Ahmed ElKordy⁽²⁾, Reham Farag⁽³⁾, Ola Abd Elbar⁽³⁾, Ahmed Faried^(4,5), Faten Y. Ellmouni^{(6)#}

⁽¹⁾Botany and Microbiology Department, Faculty of Science, Suez Canal University, Ismailia, Egypt; ⁽²⁾Botany and Microbiology Department, Faculty of Science, Sohag University, Sohag, Egypt; ⁽³⁾Department of Agricultural Botany, Faculty of Agriculture, Ain Shams University, Cairo, Egypt; ⁽⁴⁾Biology Department, College of Science and Arts, Sajir, Shaqra University, Saudi Arabia; ⁽⁵⁾Botany and Microbiology Department, Faculty of Science, Assiut University, Assiut, Egypt; ⁽⁶⁾Botany Department, Faculty of Science, Fayoum University, Fayoum, Egypt.

THE GENUS *Mangifera* L. belongs to the family Anacardiaceae, order Sapindales with 69 known species. *Mangifera indica* is an essential major tropical crop in the globe economy. This study aims to portray the significance of the usage of geometric and micrometric leaf traits to characterize Mango cultivars. Thirty-three morphological and anatomical leaf traits of 41 Mango accessions belong to six cultivars were investigated. The data were analyzed using statistical packages under R environment. Results showed that geometric and micrometric leaf traits such as the leaf length, width, petiole length, leaf blade shape, the shape of upper and lower epidermal cells, the outline of the vascular cylinder, and the number of phloem resin canals were of significance value in the characterization of Mango cultivars. Taxonomic diagnostic key based on some of those traits was constructed. ANOVAs, MANOVA, correlation, and Principal Component Analysis (PCA) retrieved the significance of applying those leaf traits as cultivar identifiers. The present investigation estimate that the attributes of the Mango leaf could be useful and straightforward cultivar identifiers that could be followed by Mango breeders to save time, efforts and money in terms of being unhindered by long juvenile stage of the tree.

Keywords: Juvenile stage, Leaf anatomy, Leaf morphology, Mango, R environment, Taxonomy.

Introduction

The genus *Mangifera* L. belongs to the family Anacardiaceae, order Sapindales (Litz & Hormaza, 2020). Kostermans & Bompard (1993) recognizes 69 species of *Mangifera* based on flower morphology. Most of these are included in two subgenera *Mangifera* L. and *Limus* (Marchand) Kosterm. The subgenus *Mangifera* contains most of the species (47) distributed into four sections: section *Marchandora* Pierre.; section *Euantherae* Pierre.; section *Rawa* Kosterm.; and section *Mangifera*

Ding Hou. A further 11 species reside in uncertain classification positions (Kostermans & Bompard, 1993). The origin and the center of *Mangifera* diversity has been established as South-East Asia and, from here it has spread and is now cultivated across the world (Bompard, 2009). According to Abdelsalam et al. (2018) *Mangifera indica* L. (Mango), was introduced for cultivation in Egypt at least 200 years ago. In 2015, the total cultivated area of Mango reached ~ 102071.76 hectares, with the main cultivation area concentrated in the Ismailia Governorate.

#Corresponding authors emails: ahmedbanhaway@science.suez.edu.eg; fyl00@fayoum.edu.eg

Received 31/8/ 2020; Accepted 19/11/ 2020

DOI: 10.21608/ejbo.2020.40870.1550

Edited by: Prof. Dr.: T. Galal, Faculty of Science, Helwan University, Cairo, Egypt.

©2021 National Information and Documentation Center (NIDOC)



The devastating flood in the arid region a consequence of rainfall and dam failure: Case study, Al-Lith flood on 23th November 2018, Kingdom of Saudi Arabia

Ahmed M. Youssef^{1,2,*}, Mazen M. Abu-Abdullah², Emad Abu AlFadail²,
Hariklia D. Skilodimou³, and George D. Bathrellos⁴

¹ Faculty of Science, Geology Department, Sohag University, Sohag, 82524, Egypt

² Applied Geology Sector, Geological Hazards Department, Saudi Geological Survey, Jeddah, 21514, Kingdom of Saudi Arabia

³ Department of Geography and Climatology, Faculty of Geology and Geoenvironment, National and Kapodistrian University of Athens, University Campus, 15784, Zografou, Athens, Greece

⁴ Sector of General, Marine Geology & Geodynamics, Department of Geology, University of Patras, University Campus, ZC 26504, Rio, Patras, Greece

* Corresponding author: amyoussef70@yahoo.com

With 11 figures and 6 tables

Abstract: On November 23, 2018, cascading rainfall events that occurred in the upstream section of wadi Al-Lith, which is located in the western part of the Kingdom of Saudi Arabia, caused a failure in the Al-Lith earthen dam. This event was followed by a large-scale devastating flood that inundated the area downstream of the dam, damaging infrastructure and property. The main scope of this work was to identify the causes of catastrophic flooding and ways to prevent and mitigate the potential consequences of a future flood occurrence in the study area. For this purpose, remote sensing images, DEM, field observations, and rainfall data were used. A geospatial integrated approach using a GIS, remote sensing, hydromorphological analysis, and rainfall-runoff modeling was utilized to provide a better understanding of the hydrology of the wadi Al-Lith catchment. Various methods were used for rainfall frequency analyses; supervised classification was applied on Landsat (OLI), in which land-use types were classified to identify the curve number values. Rainfall-runoff modeling was conducted using the catchment characteristics and rainfall analysis to calculate flood volumes and peak discharges. Peak discharge results at the flood event on November 23, 2018, and at 5- and 100-year return periods were used for the prediction of flood extent using the 2D HEC-RAS model. Water inundated depth and velocity were mapped. The result of the 5-year return period simulated model showed a good correlation with the flood extent of the event on November 23, 2018 that extracted from the sentinel-2 image. This model was validated using field observation data and remote sensing interpretation at the real flood event of November 2018. The flood model indicated that a dam failure with the substantial release of an enormous amount of water in a short period created exacerbates the problem. Also, the simulated model of the 100-year return period showed high-risk of the whole floodplain area of Wadi Al-Lith and the urbanized zone, where utterly devastation could be occurred. Finally, the results showed that a new dam proposal is urgently required to prevent the area from future flood events to replace the failed dam with a 45 m high dam. In this case, the reservoir capacity is estimated to be ~147.4 million m³, which is above the runoff volume for a 200-year return period.

Keywords: devastating floods; dam failure; inundation; Al-Lith; Kingdom of Saudi Arabia

1 Introduction

Flash floods in arid areas are often characterized by high intensity and short duration, which, when combined with the minimal response time due to fast water runoff and

lack of adequate warning systems, leads to an increase in the risk to human lives and property (Karymbalis et al. 2011, Moawad 2016, Sene 2013, Youssef et al. 2016). Extreme rainfall events are considered a crucial triggering factor causing floods and landslides, which are the

The Digital Transformation Effects in Distance Education in Light of the Epidemics (COVID-19) in Egypt

Walaa M. Abd-Elhafiez^{1,2,*} and Hanan H. Amin³

¹Mathematical and Computer Science Department, Faculty of Science, Sohag University, Sohag, Egypt

²College of Computer Science & Information Technology, Jazan University, Jazan, Kingdom of Saudi Arabia

³Information System Department, Faculty of Computers and Information, Sohag University, Sohag, Egypt

Received: 21 Sep. 2020, Revised: 22 Dec. 2020, Accepted: 24 Dec. 2020.

Published online: 1 Jan. 2021

Abstract:

On the relatively rare occasions when disaster forces schools and universities to close for a prolonged period of time, e-learning has helped fill the gap in instruction. In this paper, we study the role of digital transformation in e-learning systems in light of the global conditions resulting from the epidemics (COVID-19) in Egypt. Therefore, we focus on the importance of distance education at several factors, trying to assess the staff's response and students to new education methods and assess the distance education experience in Egyptian universities. Where the study set that various staff excited to utilize this method, unlike some of the students, who did not to accept because of their knowledge lacking.

Keywords: Distance Education, COVID-19, Digital transformation.

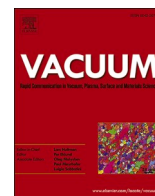
1 Introduction

Humanity knew the end of the twentieth century, and the beginning of the twenty-first as a huge revolution in the field of modern information and communication technology, which leads to a different world in terms of data, tools, text, voice, and image being transferred and dealt with via the Internet world, which creates a new world through which it can form educational environments and promote creativity in it [1]. Which made the current era characterized by amazing developments in information and communications technology field, which contributed to establishing new milestones. Modern information systems in the digital age shadow are analytical and diagnostic systems, that give broad capabilities for flexible and effective analysis, planning, and effective response to the changes surrounding the work environment. The changes are taking place in the work environment and qualify them to be more able to create and invest opportunities [2]. Educational institutions do not live alone from these global variables, especially higher education institutions where the future of universities today is related to these rapid developments in the field of knowledge and technology and the accompanying infinite flow of visions, trends, goals and

ideologies, the reality and nature of the challenges facing universities imposed many important transformations in University education systems, so any development depends on the university's ability to realize the importance of change and monitor its impacts in long and short term, and this requires the formation of highly qualified human resources as an important component of survival in the digital age[3], so it has become imperative for it. A striving to participate in making this future and defining its roles in preparing human wealth and building individuals with competence and excellence to deal with the challenges of the third millennium [4].

Since the launch of the distance education [5, 6] program, many difficulties and obstacles that may face its spread and effectiveness have started to appear: Are all students equipped with enough electronic devices (computers, tablets, smartphones) to rely on them in distance education? Do all students have a sufficiently strong internet connection that enables them to access and benefit from the lessons and programs broadcast on digital distance education channels? Do all students in villages and remote areas have access to strong internet coverage and before we talk about it, do you already own these digital devices? Has a technological infrastructure been provided

*Corresponding author e-mail: w_a_led@yahoo.com, walaa.hussien@science.sohag.edu.eg,



The effective reduction of graphene oxide films using RF oxygen plasma treatment

F.M. El-Hossary^a, Ahmed Ghitas^b, A.M.Abd El-Rahman^{c,a}, M. Abdelhamid Shahat^{b,*}, Mohammed H. Fawey^a

^a Physics Department, Faculty of Science, Sohag University, 82524, Sohag, Egypt

^b PV Unit, Solar and Space Research Department, National Research Institute of Astronomy and Geophysics (NRIAG), Helwan, Cairo, Egypt

^c King AbdulAziz University, Jeddah, Saudi Arabia

ARTICLE INFO

Keywords:

Graphene oxide (GO)
Reduced graphene oxide (rGO)
Radio frequency (RF) plasma
XPS
Raman spectroscopy
TGA
Electrical conductivity

ABSTRACT

Graphene Oxide (GO) has attracted strong research interest due to its unique mechanical, thermal, electrical, and magnetic properties. Herein, a simple oxygen plasma process is used as an eco-friendly, novel and effective surface treatment technique to enhance the microstructure, adhesion force, and electrical properties of the GO films. GO films were treated in a plasma oxygen environment at a constant RF power of 300 W and different processing times ranging from 0 to 7 min. X-ray photoelectron spectroscopy (XPS) and Raman spectroscopy are utilized to examine changes in the type of surface groups and the distribution of bonds energy before and after plasma treatment. Additionally, the effect of RF oxygen plasma treatment on other properties, such as thermal stability, surface roughness, contact angle, work of adhesion, wettability, electrical conductivity, and sheet resistance has been studied. XPS data revealed that RF oxygen plasma treatment reduced the amount of oxygen-containing groups (such as epoxides (O–C–O), carbonyls (C–O–C), and carboxyl's (O–C=O)) from 48.8% for the as-prepared GO film to 33.56% after 5 min of treatment. In addition, the average surface roughness (Ra) increased from ~7.8 of as-prepared GO film to ~8.7 μm, while the work of adhesion improved to reach 134.84 mN/m. However, with increasing plasma processing time up to 7 min, the thermogravimetric analysis (TGA) of the treated GO film showed a weight loss difference of 51.66%. Furthermore, introducing a high amount of C=O bonds (carbonyl and SP² groups of carbon atoms) after plasma treatment improved the electrical conductivity to a value of 0.156 S/m. The current results indicate that the properties of GO can be tuned by varying the degree of oxidation, which may pave the way for new developments in GO-based applications.

1. Introduction

Graphene is a monolayer of carbon atoms detached from inexpensive pure graphite that is packed into 2-D honeycomb lattices [1]. Graphene oxide (GO) is an oxygenated derivative of graphene. It has abundant functional groups of oxygen and can be exfoliated and dispersed easily in different solvents including water [2,3]. Graphene and its derivatives have enormous expectations for usage in many applications, while its low electrical conductivity is still a challenging problem. Therefore, reducing the GO sheets is considered as one of the effective ways to enhance its electrical properties. The reduced graphene oxide (rGO) has a wider range of applications than GO or even pure graphene, such as an electrode for Li-ion batteries [4], photoconductive switching [5], catalyst [6], supercapacitors [7], sensors [8], biological imaging [9], etc. As

known, GO can be chemically or thermally reduced to obtain graphene-like properties. Annealing of GO at high temperatures has used as a thermal reduction technique [10]. Likewise, the chemical reduction can be obtained using strong reducing chemicals, such as hydrazine (N₂H₄) [11] and borohydride (NaBH₄) [12]. At the same time, these reducing chemical substances are dangerous and environmental pollutants. It has been found that the rGO sheets produced by chemical or thermal reduction have more defects and poor conductivity, which reduces the carrier mobility restricting its usage in the electronic applications [13]. Alternatively, reduction by radio-frequency (RF) plasma discharge is considered as a more effective, safe, rapid reduction technique as well as an environmentally-friendly method, compared to other chemical and thermal techniques [14]. The RF plasma can be generated using a radio-frequency electric field of 13.56 MHz. In this process, with

* Corresponding author.

E-mail address: m.abdelhamid999@gmail.com (M.A. Shahat).

<https://doi.org/10.1016/j.vacuum.2021.110158>

Received 9 September 2020; Received in revised form 16 February 2021; Accepted 17 February 2021

Available online 2 March 2021

0042-207X/© 2021 Elsevier Ltd. All rights reserved.



The impact of indium metal as a minor bimetal on the anodic dissolution and passivation performance of zinc for alkaline batteries. Part II: galvanostatic, impedance spectroscopy, and charge–discharge evaluations

Mahmoud Elrouby¹ · Hoda A. El-Shafy Shilkamy¹ · Abd El-Rahman Elsayed¹

Received: 16 March 2021 / Revised: 1 June 2021 / Accepted: 24 June 2021 / Published online: 3 July 2021
© The Author(s), under exclusive licence to Springer-Verlag GmbH Germany, part of Springer Nature 2021

Abstract

The anodic dissolution and passivation processes of zinc and zinc-indium alloys were investigated in an alkaline solution of 6 M KOH using galvanostatic, electrochemical impedance, and charge–discharge measurements. Galvanostatic measurements exhibit anodic potential/time transient of the zinc anode and its alloys in the concentrated alkaline solution at different current densities. The data reveal that the passivation time ($t_{\text{pass.}}$) diminishes with increasing the content of indium in the alloy under investigation. This means that the alloying of minor indium with zinc retards its dissolution at the active region. The high oscillations in potential, which are observed in the case of zinc, disappeared with the addition of a minor indium content to zinc (Zn–In alloy). The data acquired from impedance (EIS) exhibited that the values of polarization resistance (R_p) and Warburg impedance increase, while the double-layer capacitance (C_{dl}) diminishes with increasing a minor indium content at both two investigated potentials (–500 and +500 mV vs. SCE). It is interesting to show that the inductive loop for alloys I and II at –500 mV is observed at intermediate frequencies, in addition to the capacitive loop and Warburg tail. The results of charge–discharge measurements show that the average charge–discharge separation voltages of alloys I and II are 0.8 and 0.9 V, respectively, which are higher than that of pure zinc (0.7 V) at constant time. This indicates that indium alloying with zinc leads to improvement in both energy and charge efficiency.

Keywords Zn-in alloys · Galvanostatic measurements · Impedance · Charge–discharge properties · Charge efficiency · Specific capacitance

Introduction

As the demand for energy increases in modern societies, both energy crises and environmental deterioration have encouraged the development of high-performance devices based on energy storage with non-toxic, ecologically friendly, relatively low-cost peculiarities. In energy storage research, much attention has been paid to metal–air batteries, which are considered an attractive alternative energy source for the future. Nowadays, rechargeable batteries based on metal–air have attracted

global attention [1–3]. Zinc is used as an anode material in both alkaline and chloride batteries, due to its electrochemical and environmental characteristics [4]. But, alkaline batteries are predominantly used as an efficient energy source in many electronic devices. However, zinc is highly corroded in alkaline solution, owing to its high activity [5], and this behavior remains a difficult problem. Therefore, the electrochemical and corrosion manner of zinc anode has attracted the interest of many studies in alkaline media [6–12]. The previous works showed that the dissolution process of zinc in an alkaline solution is the main cause for the appearance of oxide and hydroxide layer on its surface [11]. Besides, the zinc electrode in an alkaline battery has disadvantages during the operation such as dendritic formation through cycles, passivation of the surface, and evolution of hydrogen gas [13]. Through the charge–discharge process, the dendrite structure progressively generates and leading to a diminishing in the electrochemical

✉ Mahmoud Elrouby
dr_mahmoudelrouby@hotmail.com

✉ Abd El-Rahman Elsayed
elsayed777@yahoo.com

¹ Department of Chemistry, Faculty of Science, Sohag University, Sohag 82524, Egypt